ETHANOL DEHYDRATION WITH PROTEIN EXTRACTED CANOLA MEAL

IN A PRESSURE SWING ADSORPTION PROCESS

A Thesis Submitted to the College of

Graduate Studies and Research

in Partial Fulfillment of the Requirements

for the Degree of Master of science

in the Department of Chemical and Biological Engineering

University of Saskatchewan

Saskatoon

By

Zakieh Ranjbar

PERMISSION TO USE

In presenting this thesis/dissertation in partial fulfillment of the requirements for a Postgraduate degree from the University of Saskatchewan, I agree that the Libraries of this University may make it freely available for inspection. I further agree that permission for copying of this thesis/dissertation in any manner, in whole or in part, for scholarly purposes may be granted by the professor or professors who supervised my thesis/dissertation work or, in their absence, by the Head of the Department or the Dean of the College in which my thesis work was done. It is understood that any copying or publication or use of this thesis/dissertation or parts thereof for financial gain shall not be allowed without my written permission. It is also understood that due recognition shall be given to me and to the University of Saskatchewan in any scholarly use which may be made of any material in my thesis/dissertation.

Requests for permission to copy or to make other uses of materials in this thesis/dissertation in whole or part should be addressed to:

Head of the Department of Chemical and Biological Engineering

University of Saskatchewan

Saskatoon, Saskatchewan [S7N 5A9]

Canada

Abstract

Bioethanol is the most widely used biofuel nowadays, which can be derived from renewable sources of energy and is also environmentally friendly. The resulting ethanol from biomass, however, is as a mixture containing 10-15 wt% ethanol mixed with water and other organics. In order to be used as a fuel, the mixture should be purified to at least 99.5 wt% ethanol. Among several processes which have been applied to obtain fuel grade ethanol, adsorption using bioadsorbents seems more appealing due to low operation costs and high efficiency. In this study, canola meal after protein extraction was chosen as the biosorbent to dehydrate ethanol in a Pressure Swing Adsorption (PSA) system. The breakthrough experiments were conducted to investigate the equilibrium and kinetics of the process. The effects of temperature, pressure, feed flow rate and vapor feed concentration as well as adsorbent particle size, on the adsorption process were examined. The experimental results were compared in terms of breakthrough time, selectivity of water over ethanol and the slope of the breakthrough curve which is an indication of the mass transfer rate. The Dubinin- Polanyi model which is based on the adsorption potential theory represented a reasonable fit with the equilibrium data. The mean free energy of the adsorption process was calculated to be 0.04 kJ/ mole, which indicated the physical nature of the adsorption process.

It was demonstrated that over 99 wt% ethanol was achieved using protein extracted canola meal as the biosorbent in a pressure swing adsorption process. However, a significant amount of ethanol was also adsorbed along with water which led the selectivity of the biosorbent to adsorb water over ethanol to be less than 4.

ACKNOWLEDGEMENT

Foremost, I would like to express my sincere gratitude to my supervisors, Dr. Catherine H. Niu and Dr. Ajay K. Dalai, whose encouragement, guidance, and support from the initial to the final level of this research enabled me to develop an understanding of the subject.

I also would like to thank the members of my advisory committee: Dr. Jafar Soltan and Mr. Arcadio Rodriguez-Prado for their guidance and contribution.

I would like to acknowledge the financial support from Saskatchewan Canola Development Commission, Saskatchewan Agriculture Development Fund, and Canada Foundation for Innovation as well as University of Saskatchewan.

This thesis would not have been possible without the help and support of the members of the Chemical and Biological Engineering Department particularly Mr. Richard Blondin, Ms. Heli Eunike, Mr. Dragan Cekic, Ms Jean Horosko and Ms. Kelly Bader.

Last but not least, I am grateful to my parents for their support and motivation throughout my entire life.

Table of Contents

List of Tables

List of Figures

NOMENCLATURE AND ABBREVIATIONS

Nomenclature

C	water Content at time t (wt %)
C_0	initial Water content (wt %)
Ce	vapor feed concentration of water, (g water/cm^3)
d_p	particle diameter (m)
D_{AB}	gas- phase diffusivity (m^2/s)
Dim	diffusion coefficient for a multi component gas mixture (m^2/s)
Dij	binary diffusion coefficient of the *ij* system (m^2/s)
E	mean free energy of adsorption (kJ/mol)
i	trace component (dimensionless)
Kc	external mass transfer coefficient (m/s)
K_0	equilibrium thermodynamic constant (dimensionless)
k_1, k_2	pore constant for micropore and large pore materials (dimensionless)
M_A, M_B	molecular weights of A and B (g/mol)
n	number of components
P	pressure (bar)
P_i,	Partial pressure of the adsorbate (bar)

P^s	saturated vapor pressure of the adsorbate (bar)
q	mass adsorbed per unit mass of adsorbent (g/g adsorbent)
q_0	limiting mass for adsorption (g/g adsorbent)
q_e	equilibrium adsorption capacity, (g water adsorbed/ g of adsorbent)
R	universal gas constant (J/mol K)
T	temperature (K)
T_b	normal boiling point (1atm), K
U	superficial gas velocity through the bed (m/s)
V_b	liquid molar volume at the normal boiling point, cm^3/mol
V_c	critical volume, cm^3/mol
V_{CM}	volume of the packed canola meal (ml)
Vt	total volume of the bed (ml)
Xj	mole fraction of component j (dimensionless)
Xw	mole fraction of water in the adsorbed phase (dimensionless)
Xe	mole fraction of ethanol in the adsorbed phase (dimensionless)
Yw	mole fraction of water in the vapor phase (dimensionless)
Ye	mole fraction of ethanol in the vapor phase (dimensionless)
α	separation factor (dimensionless)
ß	affinity coefficient (dimensionless)
μ	viscosity (kg/m. s)
μ_p	dipole moment, debyes
ρ	fluid density (Kg/m^3)
Φ	void fraction (porosity) of packed bed (dimensionless)

$\sigma_{A,}\ \sigma_{B}$ characteristic Lennard- Jones (A°)

Ω_{D} diffusion collision integral (dimensionless)

$\mathcal{E}_{A},\ \mathcal{E}_{B}$ characteristic Lennard- Jones energy (J)

Ɛ adsorption potential (J/mol)

Δ coefficient related to the mean free energy of adsorption (mol^2/J^2)

ΔH° heat of adsorption (kJ/mol)

Abbreviations

APE	After Protein Extraction
BK	Breakthrough Curve
BPE	Before Protein Extraction
CM	Canola Meal
ETOH	Ethanol
FTIR	Fourier Transform Infrared Spectroscopy
HPLC	High-Performance Liquid Chromatography
MS	Molecular Sieves
PE- CM	Protein Extracted Canola Meal
PSA	Pressure Swing Adsorption
SEM	Scanning Electron Microscopy
TG/DTA	Thermo gravimetric/ Differential Thermal Analysis

1 Introduction

Many studies are carried out in different countries to find alternatives of hydrocarbon-based fuels such as gasoline, diesel fuels, etc (Kumar et al., 2010). Protection of the global environment and depletion of the conventional hydrocarbon fuel supplies have motivated researchers to develop alternative fuels including hydro, wind, biofuels, solar and geothermal energy (Frolkova and Raeva, 2010; Kumar et al., 2010). Among these proposed substitutes, biofuels have drawn more attention. Fuel- grade ethanol, biodiesel and biogas are the most promising biofuels being explored in recent times. There is an abundance of biomass on the earth which can be converted into liquid fuel. The use of biofuel is beneficial from the standpoint of the environment, energy security and economic development (Kumar et al., 2010; Ragauskas et al., 2006). Reduced carbon dioxide emissions, which are responsible for global climate change, is one of the main advantages of using biofuels instead of fossil fuels. Moreover, biofuels emit less unwanted products specially unburned hydrocarbons and carbon monoxide. These characteristics are associated with local air quality improvement. National security is also amended by using biofuels due to the reduction of petroleum net imports. Biofuels are compatible with modern vehicles so they can be used as a replacement for petroleum fuels in transportation (Hill et al., 2006; Kumar et al., 2010).

Ethanol based biofuels, which can be used as blending components with hydrocarbon-based fuels, have been considered more extensively during the last two decades (Sun et al., 2007).

1.1 Bioethanol

Having a high octane number, low emissions of carbon monoxide, volatile organic compounds and particulates make bioethanol an excellent gasoline blending component (Kumar et al., 2010).

Bioethanol is mainly produced through the fermentation of any sugar, starch or cellulose containing biomaterial (Frolkova and Raeva, 2010; Jeong et al., 2009; Kumar et al., 2010). Fermentation of biomass produces a mixture containing 8-12% v/v ethanol mixed with water and some other organics (Sun et al., 2007). Despite being totally compatible with gasoline, anhydrous ethanol could be drawn out when in contact with water and form two separate phases (Kumar et al., 2010). Therefore, the presence of water in ethanol is undesirable when blending with hydrocarbons. Consequently, there is a great interest to dehydrate ethanol in order to use it as a fuel admixture (Frolkova and Raeva, 2010). However, separation of ethanol from a large amount of water is an energy intensive process (Jeong et al., 2009). In order for ethanol to be considered as a substitute fuel, the energy obtained from ethanol should be greater than the energy consumed to produce it (Kumar et al., 2010).

1.2 Processes for production of anhydrous ethanol

The boiling points of ethanol and water at atmospheric pressure are 78.4 °C and 100 °C, respectively. But the minimum-boiling azeotrope of ethanol–water mixture is 78.2 °C at 95.6 wt% ethanol. Since the partial boiling does not change the composition of solution after azeotropic point, conventional distillation methods do not result in further purification of ethanol more than 95.6.wt% at atmospheric pressure. As a result, the remaining water should be removed through other processes (Al-Asheh et al., 2004; Kumar et al., 2010; Simo et al., 2009).

The commonly used processes for production of anhydrous ethanol constitute chemical dehydration process, dehydration by vacuum distillation process, azeotropic distillation process,

extractive distillation processes, membrane processes, adsorption processes and diffusion distillation process. Chemical dehydration process has been restrained due to considerable energy consumption and also low ethanol recovery (Kumar et al., 2010). Membrane process which was introduced as an alternative process also showed low energy efficiency (Hu and Xie, 2001). Traditional distillation process has frequently been criticized due to high energy consumption (Ladisch and Dyck, 1979; Sun et al., 2007). However, the energy efficiency can be improved by integrating a common distillation process with a pertinent adsorption system (Kim et al., 2011). One possible solution is by using distillation to obtain a 75–92 wt% ethanol-water product which is below the azeotrope (95.6 wt% ethanol), and then using adsorption to obtain anhydrous ethanol (Sun et al., 2007). Low operation costs, high efficiency, as well as a wide variety of selective sorbents make the adsorption method an appealing choice for industrial gas separation purposes. The adsorption process can be either Temperature Swing Adsorption (TSA) or Pressure Swing Adsorption (PSA). However, the latter has been used in the ethanol dehydration industry since 1980's (Kupiec et al., 2009).

2 Literature review

There are mainly two aspects which should be investigated when an adsorption process is considered; the adsorbent and the adsorption process. The first section of this chapter is dedicated to literature review on different adsorbents which have been used for ethanol dehydration while in the second section, different adsorption processes are reviewed.

2.1 Adsorbent

In order for an adsorbent material to be operative in an adsorption system, it should possess a large internal surface area attainable to the species being separated from the bulk phase (Anozie et al., 2010; Thomas and Crittenden, 1998). Furthermore, it should indicate good mechanical and kinetic properties. The former associates with resistance to attrition and strength, while the latter means being able to convey the adsorbate to the adsorption sites (Thomas and Crittenden, 1998).

Generally, adsorption of water–ethanol mixtures can be carried out in liquid or vapor phase (Frolkova and Raeva, 2010). Some of the adsorbents which are utilized in the liquid-phase adsorption process include cellulose-based materials (Frolkova and Raeva, 2010), divinylbenzene cross-linked polystyrene resins (Gulati et al., 1996; Pitt et al., 1983), silicalite (Beery and Ladisch, 2001), barley straw and wheat straw (Sun et al., 2007).

For vapor phase adsorption of ethanol-water mixtures, corn grits (Westgate et al., 1992; Westgate and Ladisch, 1993), corn meal (Chang et al., 2006a; Chang et al., 2006b; Hassaballah and Hills, 1990; Hills and Pirzada, 1989; Ladisch et al., 1984), phillipsite-rich volcanic tuffs (Colella et al., 1994), saponified starch-*g* – poly (acrylonitrile) (Pitt et al., 1983), molecular

sieves (Al-Asheh et al., 2004; Jeong et al., 2009; Kupiec et al., 2009; Simo et al., 2009), activated alumina (Beery and Ladisch, 2001), lithium chloride, and silica gel (Frolkova and Raeva, 2010) have been employed.

2.1.1 Molecular sieves

Molecular sieves which contain pores of uniform size and often consist of aluminosilicate minerals or synthetic compounds have been used as adsorbents for ethanol dehydration process. Molecular sieves have high internal porosity which makes the adsorption to occur internally. The mechanism of molecular sieve adsorption is based on diffusion of small molecules through the pores of molecular sieve while the larger molecules cannot be adsorbed. However, the surface area which is an important factor in other adsorbent materials does not play any role in molecular sieve adsorption (Kumar et al., 2010; Thomas and Crittenden, 1998).

The diameters of water and ethanol molecules are 0.25 nm and 0.40 nm, respectively. Hence, Molecular sieves with diameter of 0.3 nm allows water molecules to diffuse into the adsorbents and be retained inside while ethanol molecules are excluded from diffusing in. As a result, MS can be applied for ethanol dehydration. Small water molecules are entrapped while large ethanol molecules flow around the material. Molecular sieves can adsorb water molecules up to 22% of their weight (Kumar et al., 2010).

Sowerby and Crittenden (1988) investigated ethanol adsorption at the azeotrope composition in fixed beds packed with 0.3 nm, 0.4 nm, and 0.5 nm molecular sieves. They found that 0.4 nm molecular sieves had higher adsorption capacity than that of 0.30 nm, while 0.30 nm molecular sieves required less regeneration energy .They also found that 0.50 nm molecular sieves were unsuitable for ethanol dehydration because of adsorption of ethanol along with water molecules in the pores.

Jun- Seong Jeong et al. (2009) studied ethanol dehydration by type 3A° molecular sieves in a pressure swing adsorption system. They used two columns filled by molecular sieves to optimize a PSA system in a pilot scale.

Simo et al. (2009) used type 3A° molecular sieves in a near-adiabatic fixed bed for ethanol dehydration. They concluded that the ethanol uptake at 167 °C was about 0.03mol / kg adsorbent which was quite low compared to that of water. They also reported the selectivity of water to ethanol to be ≈ 900.

In order to regenerate the water that has been adsorbed in molecular sieves, high temperature above 200°C is required (Fahmi et al., 1999). Furthermore, molecular sieves are expensive adsorbents. Therefore, researchers have been focusing on finding more suitable adsorbents. Biomass adsorbents composed of cellulose and starch, have been found to remove water from a wide range of organics. Many studies have been carried out for using biomaterials in dehydration of ethanol. Corn, corn meal, corn grits, cellulosic materials and starch are among the most important biomaterials which have been used (Chang et al., 2006a; Crawshaw and Hills, 1990; Ladisch et al., 1984; Sun et al., 2007; Wang et al., 2010). High efficiency, less raw material cost and low energy consumption are the advantages associated with biosorbents. Their regeneration also requires less energy (Wang et al., 2010).

2.1.2 Starch-based materials

Starch-based biosorbents including corn grits, corn meal, potato starch, amylase, and maize starch have high levels of amylopectin. The mechanism of adsorption in these types of materials is based upon electrostatic forces between hydroxyl groups of the adsorbent and molecules of water (Anozie et al., 2010; Chang et al., 2006a).

Ladisch et al. (1984) investigated the ethanol dehydration in vapor phase using starch (corn and potato), xylan, pure cellulose and corn residue. They observed that corn starch and corn residue had higher adsorption capacities compared to xylan and pure cellulose due to the more concentration of amylopectin in corn starch and corn residue.

Recently, several studies have been conducted using cornmeal as bioadsorbent for ethanol dehydration (Chang et al., 2006a; Hassaballah and Hills, 1990; Hills and Pirzada, 1989; Hu and Xie, 2001; Ladisch et al., 1984). Ladisch et al. (1984) studied dehydration of ethanol using cornmeal and showed that adsorption characteristics of cornmeal did not change after 85 cycles of adsorption/desorption, and concluded that cornmeal was a stable adsorbent for ethanol dehydration.

The adsorption capacity of cornmeal varies depending on its production region. Hua et al. (2001) studied the adsorption capacities of type HI and Hb Chinese cornmeal, and found that both cornmeals had similar adsorption capacities.

Asheh et al. (2004) compared the performance of palm stone, oak and corncobs with molecular sieves, and concluded that among all the biobased adsorbents which they had used, natural palm stone had the best results in terms of breakthrough time and effluent water concentration. This bioadsorbent showed longer breakthrough time and less effluent water concentration.

Youngmi Kim et al. (2011) chose Cassava starch pearls as an adsorbent for ethanol drying due to their spherical shape, hard texture and availability. They pointed out that 80% of the starch in Cassava starch consisted of amylopectin. They compared the adsorption capacity and selectivity of Cassava starch with those of corn grits which are used in commercial scale for ethanol dehydration and concluded that Cassava starch showed better adsorption capacity compared to corn grits due to their higher surface area.

2.1.3 Cellulose-based materials

Xylan and hemicelluloses are responsible for water adsorption in cellulose-based adsorbents. Extensive research related to cellulosic adsorbents with highest degree of adsorption has not been carried out yet. However, wheat straw, barley straw and woodchips are some of the cellulosic bioadsorbents among the most important ones.

Benson et al. (2005) showed that oak chips, kenaf core, and bleached wood pulp have hydroxyl groups, which were responsible for adsorption of water molecules, and concluded that all these three materials could be used as adsorbents in an ethanol dehydration system.

Sun et al. (2007) investigated the uptakes of water and ethanol by barley straw, wheat straw and acid-washed crab shells. They observed that the water uptake of barley straw was 0.45mol/g of adsorbent, which was higher compared to those of wheat straw and acid-washed crab shells with 0.25mol/g of adsorbent and 0.02mol/g of adsorbent, respectively.

2.1.4 Other Adsorbents

Calcium oxide is among one of the first adsorbents which was used for ethanol dehydration. However, the energy consumption of adsorption process using this adsorbent was higher compared to some starchy or cellulosic materials (Ladisch and Dyck, 1979)

Ladisch et al. (1979) achieved 96.5% ethanol using sodium hydroxide as an adsorbent.

Another adsorbing agent which has been used for ethanol dehydration is activated carbon which adsorbs ethanol molecules selectively over water molecules (Kumar et al., 2010). Activated carbon derived from industrial and agricultural by-products such as palm kernel fiber, oil palm fiber, coconut husk, bamboo, etc has been demonstrated to be cheaper and more environmental friendly (Anozie et al., 2010).

Canola meal has been used as an adsorbing agent for ethanol dehydration and demonstrated the ability to dehydrate 10-95%wt ethanol-water mixture to over 99 wt% ethanol (Wickens, 2010).

2.2 Adsorption Process

Various types of systems can be designed for an adsorption process. Completely- Mixed Batch Reactors (CMBR), Completely- Mixed flow Reactors (CMFR) as well as Fixed- Bed Reactors (FBR) are the most important systems that have been used for separation processes. However, continuous- flow operations are preferable since in batch operations, the concentration of the adsorbate decreases during the adsorption process whereas, in continuous operations the concentration of the adsorbate in contact with adsorbent does not change significantly which enhances the adsorbent efficiency to separate the adsorbate (Slejko, 1985).

2.2.1 Methods

There have been numerous methods used for ethanol vapor dehydration process by adsorption. All the methods, however, are based on the following simple process: At first, ethanol –water vapor enters a column which is packed with adsorbent. Then water molecules start diffusing through the pores of the adsorbent and form a thin layer. Ethanol molecules pass through this layer to a lower level where more molecules of water are adsorbed. This process proceeds until all possible water is adsorbed. Water molecules transfer from the ethanol-water vapor to the adsorbent through a zone called mass transfer zone (Kumar et al., 2010).

Wang et al. (2010) investigated the ethanol- water adsorption using ZSG-1 adsorbent which contained sweet potato and corn as basic materials along with sticky rice, durra and crystal sugar as additives. The apparatus they used consisted of a column packed with adsorbent. Ethanol-water vapors were fed from the bottom of the column. They studied the effect of different operating conditions including temperature of the fixed bed, feed concentration and vapor

superficial velocity and determined their optimum values. They concluded that at lower superficial velocity, lower temperature and higher feed concentration, higher concentration of ethanol was obtained. The optimum conditions observed by them were at 81°C, 92.55wt% ethanol and 0.14 m/s.

Hu et al. (2001) used two types of Chinese cornmeal as adsorbing agents. A sieve plate and glass beads were used to support the adsorbents in a fixed bed. Vapor feed was provided from the bottom of the column. Karl-Fisher titration was used to define the effluent water content. By considering the plateau length and height of the breakthrough curve suitable operating conditions like vapor velocity, bed temperature and adsorbent particle size were determined. They reported the adsorption capacities of the two adsorbents as 1.40E-02 g water/g adsorbent. They also used pressurized air and silica gel bed for regeneration, and enhanced the regeneration process by using up flow fluidization which could control channeling in the bed.

Asheh et al. (2004) used palm stones (date pits), oak, and corncobs as desiccants in their study along with 0.30 nm, 0.40 nm and 0.50 nm molecular sieves which were used as reference adsorbents. Breakthrough time and effluent water content were used to investigate the performance of molecular sieves. Among different types of molecular sieves, 0.30 nm showed the highest adsorption capacity. They also found out that due to the non-uniform structure, bioadsorbents had shorter plateau time compared to molecular sieves. They also concluded that biosorbent activation did not affect the adsorption performance despite increasing the surface area.

Chang et al. (2006) studied the adsorption of water-ethanol system using cornmeal in a fixed – bed consisting temperature points. For obtaining the breakthrough curve, they collected their samples at intervals of 1 min for the first 70 min, 4 min for 70-130 min, and 5 min for 130-300

min. They studied the equilibrium and kinetic adsorption by investigating the effects of temperature, feed concentration and superficial velocity. They concluded that water selectivity over ethanol increased by increasing the superficial velocity, decreasing the ethanol vapor feed concentration and increasing the temperature. They also found out that ethanol-water adsorption over cornmeal was a diffusion –limited process.

Jeong et al. (2009) used pressure swing adsorption process using zeolite as an adsorbent in order to dehydrate ethanol-water mixture. Their apparatus comprised of two columns, and the concentration of the product was determined by a Karl-Fisher titrator. They first carried out a breakthrough experiment for feed flow rate of 51.7 Nm^3/hr, feed concentration of 93.2 wt% at 2.5-3.0 atm and 130-135^oC, to understand the phenomenon that developed during the adsorption process and then they obtained maximum productivity for different feed flow rates in order to attain the optimum operating conditions.

Kim et al. (2011) used a glass column packed with cassava starch in the form of spherical pellets. The column was equipped with a water jacket. CO_2 gas was used at temperature of 105°C and superficial velocity of 5.60 m/min for the regeneration process. The effluent concentration during the adsorption cycle was controlled online using a density meter, while the composition of the regenerant condensate was monitored by GC equipment. The adsorption performance of the cassava pearls was presented in terms of adsorption capacity and selectivity of the adsorbent and was compared to those of corn grits which are currently being used commercially for ethanol dehydration. They concluded that cassava starch pellets showed higher adsorption capacities compared to corn grits with the same particle size, which could be due to the higher surface area of the cassava starch pearls. The material has shown a potential for commercialization.

Simo et al. (2009) have conducted their experiments using a pilot scale near adiabatic stainless steel column supplied with six heat tapes to provide constant temperature along the column. W. R. Grace 3A zeolite was used as an adsorbent in a Pressure Swing Adsorption (PSA) system. The pressure of the system was kept constant during the experiments using a pressure regulator. Nitrogen gas was utilized as a carrier and also purging gas. They carried out their experiments in the temperature range of 100-200 °C and pressure range of 2-6.70 bars. The effects of temperature, pressure, pellet size, and flow rate as well as water concentration were investigated to determine the controlling mass transfer mechanism.

2.2.2 Mechanism

Mainly there are three mass transfer resistances controlling the uptake of an adsorbent: (1) A laminar film surrounding the pellet known as external film resistance. (2) Transfer of adsorbate molecules from the surface of the adsorbate to the micropores known as macropore resistance (3) Micropores through which the adsorbate diffuses inside the particle. The rate controlling mechanism, however, can be specified by investigating the effect of operating conditions, since each mechanism is dependent on a specific operating condition (Simo et al., 2009).

In a Temperature Swing Adsorption system used by Sowerby et al. (1991), external fluid and micropore diffusion were considered to be the rate-controlling mechanisms since the system showed a strong temperature and concentration dependence.

Kupiec et al. (2003) concluded that in the isothermal adsorption of ethanol-water system, micropore diffusion was the rate – controlling mechanism.

Eigenberger et al. (2004) investigated the ethanol-water adsorption on W. R. Grace 4A zeolite.10 for temperatures in the range of 25 to 80 °C and pressures between 2 to 5 bars. They concluded that macropore diffusion was the rate controlling step.

Simo et al. (2009) studied the contribution of the three different mass transfer resistances in a pilot scale near- adiabatic fixed bed apparatus using W.R. Grace 3A zeolite. They calculated the individual mass transfer resistances for each experimental run, and shown that the adsorption process was dominated by micropore and macropore resistances while the external mass transfer resistance showed only a small contribution to the overall mass transfer resistance.

2.2.3 Adsorption Isotherm

An adsorption system reaches a state called equilibrium in which no net adsorption takes place. Adsorption isotherm relates the amount of substance adsorbed at equilibrium to the concentration of adsorptive species in the solution at constant temperature. Various isotherm models such as Langmuir, Brunauer- Emmett- Teller (BET), Gibbs, Freundlich, linear and adsorption potential theory model have been considered to describe adsorption isotherms (Slejko, 1985).

Ladisch et al. (1984) used Henderson's equation to describe adsorption isotherms on cornmeal at 40 to 100 ° C. Chang et al. (2006) studied the adsorption isotherm of cornmeal at temperature range of 82- 100°C and presumed that Polanyi adsorption potential theory, Sircar's model and Henry's model gave the most reasonable fit to their experimental data. Breakthrough curves and mass transfer diffusivity were determined using isotherms in their study. Asheh et al. (2004) obtained adsorption capacity of different biosorbents by fitting the Guggenheim, Anderson, and De Boer (GAB) model to their experimental data.

2.2.4 Effects of Operating Conditions

2.2.4.1 Temperature

Temperature has a significant effect on the adsorption capacity of an adsorbent. On one hand, at higher temperatures adsorbate diffuses faster into the adsorbent, on the other hand, equilibrium capacity of the adsorbent changes at higher temperatures (Slejko, 1985).

Wang et al. (2010) studied the effect of temperature in a ethanol- water adsorption system at 81^{o}C and 89^{o}C, and concluded that 100% ethanol in the effluent was acquired at 81 ^{o} C. Moreover, by developing breakthrough curves they noticed that at 89^{o}C the plateau length of the breakthrough curve was shorter, and they came to the conclusion that adsorption was more favorable at lower temperatures.

Hua et al. (2001) carried out experiments to investigate the effect of temperature in a fixed bed by determining breakthrough curves at 82, 87, 94, and 100°C. They observed that the plateau length of the breakthrough curves were shorter at higher temperatures except at 82°C due to the reflux of the condensate at this temperature.

Chang et al. (2006) set up seven temperature points along a 90 cm column and used a multimode heat-resistance contact thermometer to measure the temperature at each point. The operating temperature, however, was considered to be the average temperature over them. They concluded that separation factor and selectivity for water increased by increasing the temperature.

2.2.4.2 Vapor Feed Concentration

Wang et al. (2010) investigated the effect of feed concentration on the adsorption performance, and concluded that by increasing the ethanol feed concentration, the ethanol product concentration increased due to the fact that when less water was adsorbed, less temperature was released and adsorption capacity increased at lower temperatures.

Anozie et al. (2010) studied the effect of initial water concentration on selectivity of water over ethanol, adsorption capacity and water removal efficiency and concluded that by increasing the initial water concentration, water removal efficiency and water selectivity decreased, while the adsorption capacity first increased and then started to decrease.

By obtaining breakthrough curves for three different types of molecular sieves, Asheh et al. (2004) concluded that higher water concentration in the feed resulted in shorter breakthrough time and higher water concentration in the effluent.

Chang et al. (2006) investigated the effect of feed concentration in an ethanol dehydration process and concluded that as the ethanol feed concentration increased, adsorption selectivity decreased and separation factor increased. Productivity, on the other hand, increased by increasing the ethanol concentration, but started to decrease at higher ethanol concentrations since ethanol provided a resistance to water adsorption.

2.2.4.3 Feed Flow Rate

Low superficial velocities corresponding to low feed flow rates cause low mass transfer rate, whereas high superficial velocities lead to increase in pressure drop. Consequently, there has to be an optimum for bed superficial velocity in an adsorption system (Cooper and Alley, 2002).

Wang et al. (2010) investigated the effect of vapor superficial velocity in a fixed bed using an adsorbent called ZSG-1. They used two velocities of 0.14 m/s and 0.30 m/s, and found that higher concentration of ethanol was obtained using lower superficial velocity of 0.14m/s.

Hu et al. (2001) used a fixed bed packed with cornmeal. They developed breakthrough curves at different bed velocities of 4.40, 6.10 and 9.90 cm/s and concluded that ethanol concentrations more than 99.50 wt % could be obtained at bed superficial velocity of 6.10 cm/s.

Chang et al. (2006) carried out their experiment for both equilibrium and kinetic adsorption using a column packed with cornmeal, and found that increasing the bed superficial velocity increased the water selectivity, which was defined as water percentage in the total amount adsorbed.

2.2.4.4 Particle Size

Hu et al. (2001) used three sizes of cornmeal: <40 mesh, 40–60 mesh, and 60–100 mesh, and obtained breakthrough curves. They found that particles in the range of 60-100 mesh showed the best adsorption performance while using smaller particles with the size of more than 100 mesh decreased the adsorption capability due to a higher pressure drop. Anozie et al. (2010) used four groups of particle sizes and concluded that adsorbents in the form of powder depicted a better adsorption performance.

Asheh et al. (2004) used three types of molecular sieves: 0.30 nm, 0.40 nm and 0.50 nm and concluded that 0.30 nm molecular sieves had the longest breakthrough time and highest product ethanol concentration due to their highest surface area.

2.2.4.5 Pressure

Although Pressure Swing Adsorption (PSA) is the method currently being used for ethanol dehydration in the industry, there is very limited information in the literature regarding the investigation of the effect of pressure on the adsorption/desorption process.

Simo et al. (2009) studied the effect of pressure in a near- adiabatic fixed bed using molecular sieves as adsorbent. They conducted their experiments at temperature of 167°C for three different pressures of 224, 448 and 689 Kpa, and concluded that the macropore resistance which was controlled by molecular diffusion mechanism was the governing mechanism. They also found that the rate of the regeneration process was not influenced significantly by the change of the pressure.

3 Knowledge Gaps and Objectives

3.1 Knowledge Gap

This research project emphasizes on ethanol dehydration by using bioadsorbents in a Pressure Swing Adsorption (PSA) process which is the common method being used in the ethanol dehydration industry since 1980's. The commercial 3-A molecular sieves which are being used in ethanol dehydration industry have low water uptake of 0.20 g /g dry adsorbent. They also need high temperature in the range of 190-210 °C for dehydration. However, there has been an extensive research on using bioadsorbents for ethanol dehydration process and it has been reported that corn grits have been used for ethanol dehydration in the industry, which shows the bioadsorbents' potential to be commercialized in this application. However, using this biomaterial as an adsorbent can place pressure on food consumption.

A potential biomaterial which can be used as an adsorbent for ethanol dehydration is canola meal. According to Statistic Canada, 14 million tons of canola was produced in Western Canada in the year 2011. Canola meal, however, is one of the byproducts of canola industries including oil extraction and biodiesel production. The commercial price of canola meal is $ 0.24 /Kg in the year 2011, which is much cheaper compared to that of molecular sieves which is 3-120 $/ Kg. Canola meal is composed of 36% crude protein, 12% moisture, 20% neutral detergent fiber consisting of cellulose, hemicellulose and lignin, 5% starch, 10% free sugar and non-starch polysaccharides, 4% crude fat, and 6% ash (Canola council of Canada, 2011). However, the protein content of canola meal is reported to have well balanced amino acid composition which can be used for human consumption. This makes canola meal be an important protein source; as a result, canola meal residues after protein extraction will become an abundant by-product.

Baylak et al. (2012) have used raw canola meal as an adsorbent for ethanol dehydration. They demonstrated that canola meal was capable of removing water selectively from ethanol due to the presence of cellulosic based materials a majority of which still remains after canola meal protein extraction. Therefore, there is an extensive incentive to investigate the capability of protein extracted canola meal as a bioadsorbent in an ethanol dehydration process in order to make use of this cost-effective material. Ideally, the exhausted protein extracted canola meal after ethanol dehydration will still be usable for animal feed and/or a feedstock for bioethanol production through fermentation as it is rich in cellulosic components. The immediate benefits of canola meal commercialization as an adsorbent in the ethanol dehydration industry consist of decreasing the ethanol production cost in the Saskatchewan ethanol industry and enhancing the Saskatchewan agricultural industry by selling their waste products. Furthermore, increasing the ethanol production rate will benefit the environment.

Despite being the most common method for ethanol dehydration in the industry since 1980's, Pressure Swing Adsorption (PSA) method with protein extracted canola meal as adsorbent has never been studied extensively by researchers, and there is limited information in the literature regarding the performance of a Pressure Swing Adsorption (PSA) system.

Based on the discussion above, the knowledge gaps in the ethanol dehydration process are as follows:

- Canola meal consists of fibre, soluble non-structural carbohydrates, phytate, minerals and 35-42% protein with a well balanced amino acid composition which can be used for human consumption (Milton Bell and Keith, 1991; Tan et al., 2011). The adsorption

capacity of protein extracted canola meal for ethanol dehydration has not been studied systematically.

- There is no information in the open literature on the effect of different operation conditions on the dynamic adsorption of protein extracted canola meal as an adsorbent in a Pressure Swing Adsorption (PSA) system.

- The adsorption isotherm for protein extracted canola meal in an ethanol dehydration process has never been discussed.

- The stability of protein extracted canola meal as an adsorbent for ethanol dehydration has never been addressed before.

3.2 Research Objectives

The overall objective of this research is to determine the capability of protein extracted canola meal for ethanol dehydration in a pressure swing adsorption process.

3.2.1 Sub-objectives

- Characterize the biosorbent by determining the functional groups using FT-IR, the composition of the biomass through Ultimate/Proximate, kjeldahl and ICP-MS analyses, the bioadsorbent morphology using SEM images and devolatilization characteristics of the biomass with temperature by TG/DTA.
- Examine the dynamics of ethanol dehydration by protein extracted canola meal in a Pressure Swing Adsorption (PSA) process at different pressure, temperature, flow rate, and feed concentration as well as bioadsorbent particle size.

- Determine the adsorption capacity of water/ethanol on protein extracted canola meal in a PSA process.
- Demonstrate the equilibrium uptake of water/ ethanol on the bioadsorbent.
- Evaluate the regeneration process and stability of protein extracted canola meal as an adsorbent.

4 Materials and Methods

4.1 Biosorbent Preparation

Brassica Juncea variety of protein extracted canola meal was supplied from BioExx Specialty Proteins Ltd, Saskatoon, Canada. The meal was dried for 24 hrs in an air- convection oven at 105°C, then it was ground and sized by Canadian Standard Sieves Series (Combustion Engineering Canada Inc.) to give particles with diameters of less than 0.43 mm, 0.43- 1.18 mm and bigger than 1.18mm. The canola meal with the particle size of 0.43-1.18mm was used for the experiments based on the surface area and ease of operation in the column. Cylindrical pellets of canola meal with diameter of 5 mm were made using a California Pellet Mill (CPM-Laboratory Model CL-5, California Pellet Mill Co., Crawfordsville, IN)

4.2 Biosorbent Characterization

The biosorbent was characterized by determining the functional groups using FT-IR 4100, the composition of the biomass through Ultimate/Proximate, kjeldahl and ICP-MS analyses, the bioadsorbent morphology using SEM images and the devolatilization characteristics of the biomass with temperature by a PerkinElmer instrument, Pyris Diamond TG/DTA.

Proximate analysis

Moisture, ash and volatile content of canola meal were determined according to ASTM methods. The moisture analysis was carried out using the procedure given in ASTM 3173-87 (2003). The ash content was determined according to ASTM 3174-04 (2004). A crucible containing 5 g of sample was placed in a muffle furnace (Holpack, USA) for 4 h at temperature of 575±10 °C. Then the crucible was pulled out of the furnace and put in a desiccator to cool down. The

remaining residue in the crucible is the ash content which is a total amount of minerals in the sample.

The volatile content of the sample was measured by following the procedure of ASTM D 3175-07 (2007). 5 g of sample was placed in the muffle furnace at 950±10 °C for 7 min. The crucible containing the sample was weighted after it had been put in the desiccator to cool down. The weight loss of the sample is attributed to the volatile matter.

Ultimate Analysis

To determine the elemental composition of the biosorbent in wt% of carbon, hydrogen and nitrogen as well as sulfur, the ultimate analysis was performed by using a PerkinElmer Elemental CHNS analyzer. 4-6 mg of sample was put in a tin boat which was placed in the analyzer after being fold properly. Sample is burnt in an excess of oxygen in the analyzer and the combustion products are collected in several traps and used to estimate the composition of the sample.

ICP-MS

ICP-MS analysis was used to quantify some common elements including Na, Mg, P, K and Ca in the biosorbent.

Kjeldahl method

The protein content of canola meal before and after protein extraction was determined by kjeldahl method (Ghodsvali et al., 2005).

Thermo gravimetric/ Differential Thermal Analysis (TG/DTA)

To study the devolatilization characteristics of the biosorbent with temperature, TG/DTA analysis was performed using a PerkinElmer instrument, Pyris Diamond TG/DTA. The

devolatilization characteristics of the biosorbent were investigated in the range of 22°C to 400°C at the rate of 5 °C/min.

Scanning Electron Microscopy (SEM)

To investigate the effect of protein extraction on the external morphology (texture) and crystallinity of the biosorbent, images were taken using scanning electron microscopy (SEM, Model JEOL 840A, GELLAR dPICT Acquisition System). All the images were acquired at 25 kV.

Fourier transform infrared spectroscopy (FTIR)

In order to evaluate the effect of protein extraction on the functional groups of the biosorbent, the FT-IR analysis was performed. The FT-IR spectra of biosorbent were obtained using a FT-IR 4100. A mixture containing 5 mg of the biosorbent and 100 mg of dry KBr was pressed into a disk to prepare pellets. Each spectrum was taken in the IR range of 450- 6000 cm^{-1} at a resolution of 16 cm^{-1}.

4.3 Feed Solution Preparation

Ethanol solutions with different concentrations were prepared by mixing 200proof ethanol (reagent grade, Commercial Alcohols Inc., Canada) and distilled water.

4.4 Adsorption/ Desorption Experiments

The adsorption experiments were carried out in the experimental set up shown in Figure 4.1. The adsorption system consists of a stainless steel fixed bed column with dimensions of 500 mm long (inside), 47.50 mm ID, and 1.65 mm wall thickness. An oil heating jacket is used to maintain the temperature of the column constant during the adsorption process. The feed solution which is stored in a sealed container is pumped by using a Cole- Parmer, RK-74930-05 pump to a nebulizer in which it is mixed with nitrogen gas which is used as a carrier gas. Nitrogen gas is

supplied from a pressure cylinder. After being broken up to small aerosol droplets in the nebulizer, the mixture passes through tubing which is equipped with Cole- Parmer heating tapes (50-60Hz, 120 V, 624W, 5.20A). The rest of the tubing before the column is placed in an oil bath to further increase the temperature of the mixture and ensure the complete vaporization. It should be noted that the presence of liquid in the column makes the biosorbent to swell and lose some of its capacity; therefore, the liquid feed should be vaporized thoroughly prior to entering the column. The vapor feed enters the column from the top through a three-way valve. Temperature is controlled at the top and bottom of the column by two thermocouples (Omega K type, US) which are attached to Omega DPI32 outputs. A back pressure regulator is used to maintain isobaric operation during the adsorption process. The pressure of the column at the bottom is controlled by a pressure transducer (Honeywell, US) attached to a DPIS32 output. After passing through the fixed bed column, the dry product stream is condensed in a condenser and collected by a Gilson FC 203B fraction collector. The product samples are collected at intervals of 2 min for the first 10 min, 5 min for 45 min, and 10 min for the rest of the experiment.

The adsorption process was terminated when the bed reached its maximum adsorption capacity. The bed was considered saturated when the temperatures at the top and bottom of the bed reached the inlet temperature of the vapor.

After the adsorption process is completed, the regeneration process is started by discharging the vapor feed from the top of the column and passing the nitrogen gas as a purging agent at 1.22 L/ min for 4 hrs from the bottom of the column while the pressure is lowered to the vacuum. The regeneration product is collected through a condenser which is attached to the top of the column.

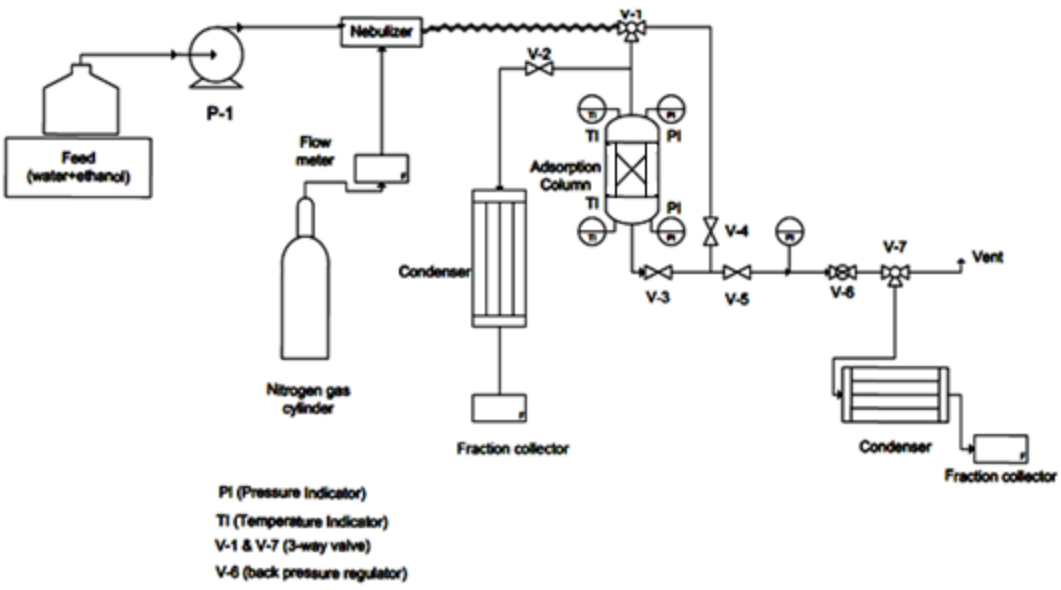

Figure 4.1: Schematic diagram of the experimental set-up

4.4.1 Dynamic Study

To study the effect of operating conditions on the adsorption performance, breakthrough curves which are plots of relative concentration(C/C_0) versus time, where C is water concentration at time t and C_0 is the initial water concentration, and also ethanol concentration versus time are used. The breakthrough time is designated to be the time when the ethanol content in the effluent equals 99%.

The effects of vapor feed flow rate at 3 ml/min and 6 ml/min, ethanol feed concentrations of 80wt % , 85wt % , 90wt % , and 95wt % , initial pellet temperatures at 90°C, 95°C, and 110°C, and total pressure at 20 psig and 5 psig as well as adsorbent particle sizes of 0.43- 1.18 mm in the powder form and cylindrical pellets of 5 mm diameter are investigated to determine the operating conditions at which the adsorption column has its best performance.

In order to evaluate the effect of external mass transfer on the adsorption, the external mass transfer coefficient is calculated according to the Thoenes- Kramers correlation (Fogler, 2006)

$$Kc = \left[\frac{U d_p \rho}{\mu(1-\Phi)}\right]^{\frac{1}{2}} \left[\frac{\mu}{\rho D_{AB}}\right]^{\frac{1}{3}} \left[\frac{D_{AB}(1-\Phi)}{d_p \Phi}\right] \quad (4.1)$$

Where U= superficial gas velocity through the bed (m/s)

μ=Viscosity, kg/m. s

ρ= fluid density, Kg/m^3

d_p= particle diameter, m

D_{AB}= gas- phase diffusivity, m^2/s

Φ= void fraction (porosity) of packed bed

The particle diameter (d_p) is defined as equivalent diameter of sphere of the same volume. However, since the adsorbent particles used in this study were in the form of powder in the range of 0.43- 1.18 mm, d_p was considered to be the median particle diameter of 1.18 mm estimated by a Malvern Mastersizer- S Long Bench size distributor. To study the effect of the particle size of the adsorbent, pellets with diameter, d_p, of 5 mm were used.

The values of gas viscosity and density were obtained from HYSYS software.

The void fraction (porosity) of the packed bed was evaluated as follows:

$$\emptyset = \frac{V_t - V_{CM}}{V_t} \quad (4.2)$$

Where Vt is the total volume of the bed and V_{CM} is the volume of the packed canola meal.

The binary gas phase diffusivity, $D_{AB,}$ is estimated through Chapman and Enskog equation (Poling et al., 2001):

$$D_{AB} = \frac{0.00266\, T^{\frac{3}{2}}}{P M_{AB}^{\frac{1}{2}} \sigma_{AB}^2 \Omega_D} \quad (4.3)$$

Where $M_{AB} = 2[\,(1/M_A) + (1/M_B]^{-1}$

M_A, M_B= molecular weights of A and B

P= pressure, bar

T= temperature, K

σ_{AB} = characteristic length of the intermolecular force law, A°

ΩD= diffusion collision integral

σ_{AB} is estimated as:

$$\sigma_{AB} = (\sigma_A \sigma_B)^{\frac{1}{2}} \quad (4.4)$$

Where σ is the characteristic Lennard- Jones length and is calculated as follows: (Poling et al., 2001)

$$\sigma = \left(\frac{1.585 V_b}{1+1.3\delta^2}\right)^{\frac{1}{3}} \quad (4.5)$$

$$\delta = \frac{1.94*10^3 \mu_p^2}{V_b T_b} \quad (4.6)$$

V_b is the liquid molar volume at the normal boiling point, cm^3/mol:

$$V_b = 0.285\, V_c^{1.048} \quad (4.7)$$

Where V_c is the critical volume, cm^3/mol

T_b is normal boiling point (1atm), K

μ_p is dipole moment, debyes

Ω_D is evaluated according to Neufield et al. (1972) (Poling et al., 2001),

$$\Omega_D = \frac{A}{(T^*)^B} + \frac{C}{\exp(DT^*)} + \frac{E}{\exp(FT^*)} + \frac{G}{\exp(HT^*)} + \frac{0.19\delta_{AB}^2}{T^*} \quad (4.8)$$

Where $T^* = KT/\varepsilon_{AB}$ $A=1.06036$ $B=0.15610$

$C=0.19300$ $D=0.47635$ $E=1.03587$

$F=1.52996$ $G= 1.76474$ $H=3.89411$

ε_{AB}/k is defined as:

$$\frac{\varepsilon_{AB}}{K} = \left(\frac{\varepsilon_A}{K}\frac{\varepsilon_B}{K}\right)^{1/2} \quad (4.9)$$

Where ε/K is calculated as follows (Poling et al., 2001):

$$\frac{\varepsilon}{K} = 1.18(1 + 1.3\delta^2)T_b \quad (4.10)$$

For a ternary mixture, the diffusion coefficient is calculated by Blanc's law (Poling et al., 2001),

$$D_{im} = \left(\sum_{\substack{j=1 \\ j\neq i}}^{n} \frac{X_j}{D_{ij}}\right)^{-1} \quad (4.11)$$

Where *i* is the trace component, and *Xj* is the mole fraction of component *j*.

Water is considered as the trace component in this case. After calculating the binary gas phase diffusivities according to Equation 4.3, the overall diffusivity is calculated by Equation 4.11.

In this study, the breakthrough time is designated to be the time when the water content in the effluent reaches 1 wt%.

Water or ethanol uptake which is defined as water/ ethanol adsorbed per kg of packed dry adsorbent at the breakthrough point was determined by the amounts of water/ ethanol input to the column minus the accumulated amounts of water/ ethanol in the effluent at the breakthrough point being divided by the dry net weight of the protein extracted canola meal.

4.4.2 Adsorption Isotherm

The adsorption isotherms are determined at three different temperatures of 90°C, 95°C and 110°C. The narrow range of the operating temperatures is due to the vapor feed condensation at lower temperatures and damage to the adsorbent at higher temperatures. The adsorption system is considered to reach equilibrium or be saturated when the water content in the effluent equals that in the feed. The adsorption capacity of the adsorbent at equilibrium which is defined as mole water/ ethanol adsorbed per kg of packed dry adsorbent is calculated by the total amount of water input to the system minus the total amount of water in the effluent at equilibrium being divided by the dry net weight of the canola meal. The experimental data is fitted into Adsorption Potential Theory model for micropore and large pore materials to see which one is a better representative for the adsorption isotherm in this system.

Baylak et al. (2012) observed that a significant amount of ethanol was adsorbed by canola meal along with water. Therefore, it is of great importance to quantify water selectivity over ethanol by defining a separation factor as (Chang et al., 2006b).

$$\alpha = \frac{X_w/X_e}{Y_w/Y_e} \tag{4.7}$$

Where *Xw* and *Yw* are the mole fractions of water in the adsorbed phase and the vapor phase, respectively, and *Xe* and *Ye* are the corresponding ethanol mole fractions.

4.5 Data Analysis

The water content for each sample in the effluent is determined by an automated Karl-Fischer Titrator (Titroline KF, Schott Instruments). The ethanol content is calculated by subtracting the total mass of the sample by the mass of water. The ethanol content obtained by this method is in agreement with that achieved from HPLC (Agilent, 1100 Series, Refractive Index Detection)

5 Results and Discussion

5.1 Biosorbent Characterization

The composition of canola meal before and after protein extraction was determined through ultimate, proximate, ICP-MS as well as Kjeldahl analyses. The results are displayed in Table 5.1 and 5.2. BPE and APE denote canola meal before and after protein extraction, respectively.

Table 5.1: Major composition of canola meal before and after protein extraction

Canola meal	Moisture content (wt %)	Ash content (wt %)	Volatile matter (wt %)	Protein Content (%)*
BPE**	5.61± 0.20	6.30± 0.11	79.42± 2.90	36.98± 0.38
APE***	5.41± 0.19	4.54± 0.00	87.01± 0.56	33.00±1.68

*Protein content was determined by kjeldahl method (Ghodsvali et al., 2005). **Before Protein Extraction;*** After Protein Extraction

As it can be seen from Table 5.1, the moisture content of the canola meal remained constant after protein extraction, while there was a slight change in the protein, ash and volatile contents. It should be noted that a significant amount of protein still remained in the canola meal after protein extraction. The remaining protein content is determined by the protein extraction efficiency of the current industry, in this case by BioExx, Saskatoon.

Table 5.2: ICP-MS analysis

	Na (ppm)	Mg(ppm)	P (ppm)	K(ppm)	Ca (ppm)
BPE*	40	7198	13430	15608	8246
APE**	5900	4128	5854	5741	8227

*Before Protein Extraction;** After Protein Extraction

According to Table 5.2, after protein extraction, the Na content increased considerably while the amount of Mg, P and K decreased and the Ca content remained almost the same.

Canola Council of Canada (Canola Council of Canada, 2011) reported the moisture and ash content of the raw canola meal as max 12% and 6.10%, respectively. According to Canola Council of Canada (2011), canola meal consists of 20% neutral detergent fiber comprising cellulose, hemicelluloses and lignin, 5% starch and 10% free sugar and non-starch polysaccharides. Canola meal has a complex carbohydrate matrix. The cellulose owns a crystalline structure with microfibrils which are linked together by hydrogen bonding and are enclosed by amorphous hemicelluloses. The lignin plays a major role in sticking the other components together.

The major mechanism responsible for water adsorption by canola meal is the polar interaction between water molecules and the hydroxyl groups connected to the polysaccharides. However, the hydroxyl groups which are located inside the microfibrils structure are not available for water adsorption.

The devolatilization characteristics of canola meal obtained from TG/DTA analysis before and after protein extraction are depicted in Figure 5.1. As it can be seen, the onset temperature, the temperature at which the weight loss begins, is in the range of 200°C to 250°C for both materials.

Raveendran et al. (1996) associated the devolatilization behavior of biomass to the presence of cellulose, hemicelluloses and lignin. Biagini et al. (2006) investigated the devolatilization of hemicelluloses, cellulose and lignin. They reported the onset temperature of these chemical

constituents to be 253°C, 319°C and 253°C, respectively. They also observed that lignin decomposed in a wider range of temperature.

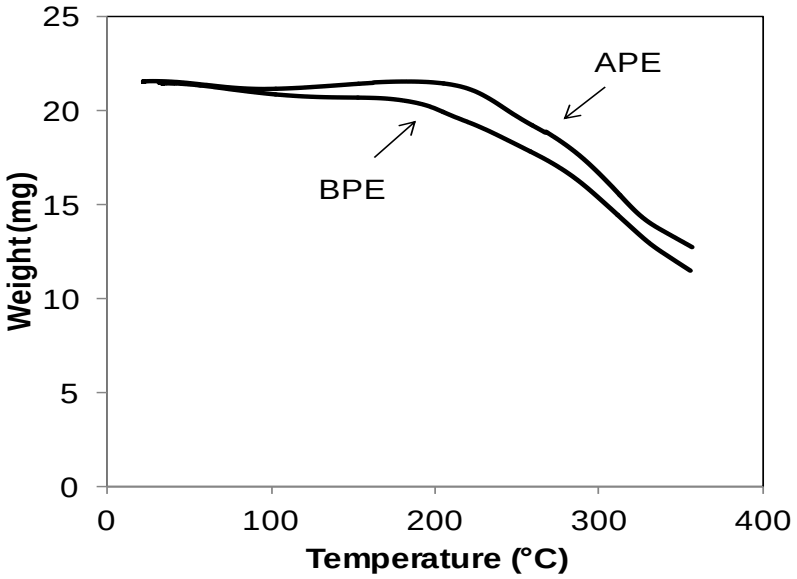

Figure 5.1: TG/DTA analysis of canola meal before and after protein extraction. BPE and APE denote canola meal before protein extraction and after protein extraction, respectively.

The weight loss at temperatures lower than 100°C can be attributed to the loss of easily volatiles, while the weight loss at 100- 130°C is due to loss of water, loss of volatile compounds correspond to 130-250°C, hemicelluloses is lost at 250-350°C and cellulose and lignin are lost at> 350°C.

The FT-IR analysis was carried out to determine the major functional groups present in canola meal as well as to evaluate the effect of protein extraction on the functional groups. As it can be noted from Figure 5.2, there is no considerable change in the functional groups before and after protein extraction.

The most noticeable peaks in the spectrum are associated to be –OH stretching vibration (3423 cm^{-1}), CH_2 and CH_3 asymmetric and symmetric stretching vibrations (2915 cm^{-1}), C-N stretch (1051 cm^{-1}) and C=O amid (1655 cm^{-1}). The first two functional groups are related to the presence of cellulose, hemicelluloses and lignin (Himmelsbach et al., 2002).

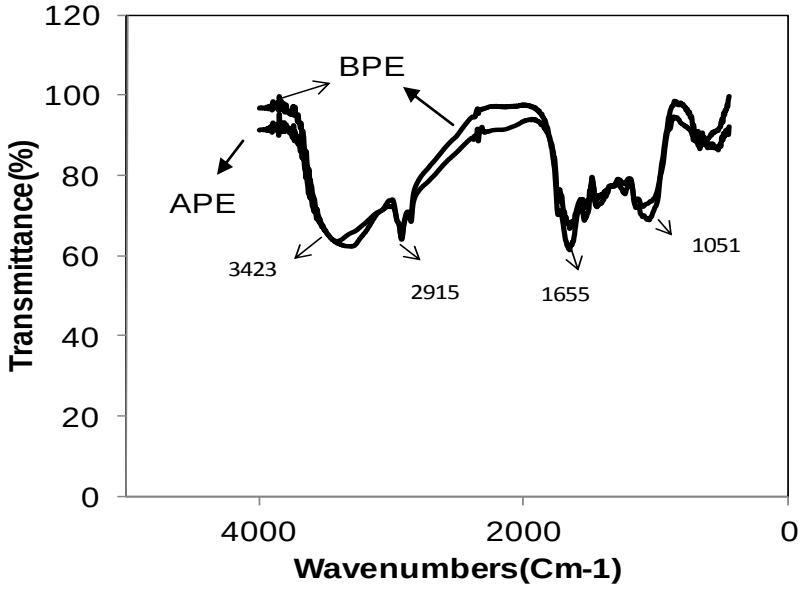

Figure 5.2: FT-IR analysis of canola meal before and after protein extraction. BPE and APE denote canola meal before protein extraction and after protein extraction, respectively.

Surface images of the biosorbent before and after protein extraction at resolutions of 1μm and 10 μm are provided in Figure 5.3. Comparing the images before and after protein extraction, it can be deducted that the morphology of the canola meal did not change significantly by protein extraction and the size and shape of the particles remained almost the same.

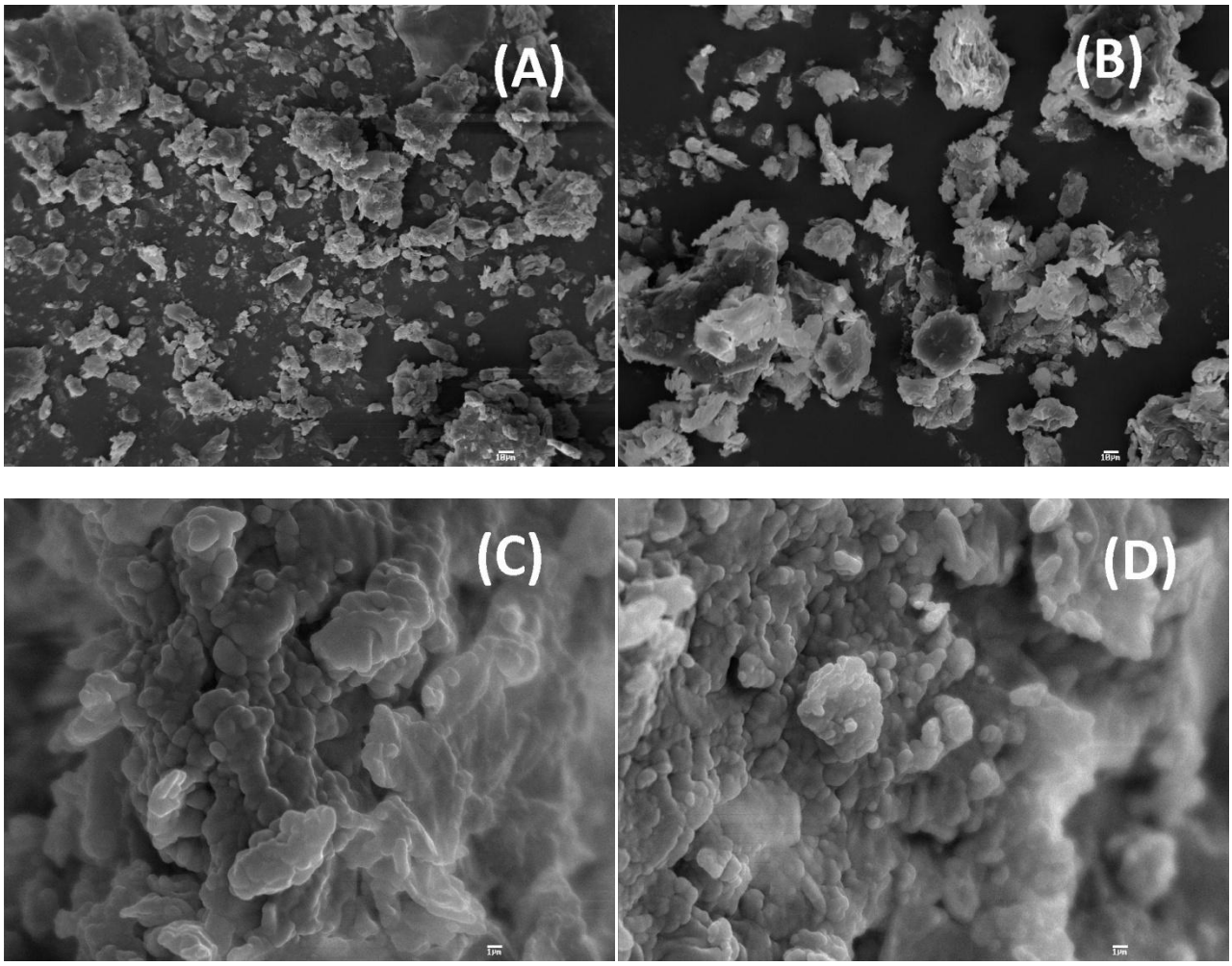

Figure 5.3: Scanning Electron Microscopy (SEM) images of canola meal. (A) Canola meal before protein extraction at 10 μm. (B) Canola meal after protein extraction at 10 μm. (C) Canola meal before protein extraction at 1 μm. (D) Canola meal after protein extraction at 1 μm.

5.2 Reproducibility Study

Reproducibility of the experimental data was investigated. Three random experiments at different pressures and temperatures are presented here as example.

Table 5.3 summarizes the operating conditions for the selected experiments.

Table 5.3: Operating conditions for the selected experiments

Group number	Temperature(°C)	Pressure(Psig)	ETOH feed conc. (wt %)	Feed flow rate(ml/min)	CM particle size(mm)
1	95	5	95	3	0.43-1.18
2	95	20.50	95	3	0.43-1.18
3	90	20.50	95	3	0.43-1.18

The replicates are compared in terms of water and ethanol uptakes at equilibrium as well as selectivities, as shown in Table 5.4- 5.6. The water and ethanol breakthrough curves are also compared in Figures 5.4 -5.6.

Table 5.4: Uptakes and selectivities for duplicate runs at experimental condition #1

	1	2	Average	STDV	Coefficient of Variation (%)
Water uptake*	11.31E-03	11.43E-03	11.37E-03	8.77E-05	0.77
Ethanol uptake*	8.78E-02	8.73E-02	8.76E-02	2.85E-04	0.32
water selectivity	2.43	2.45	2.44	1.47E-02	0.60
Ethanol selectivity	4.11E-01	4.07E-01	4.09E-01	2.46E-03	0.60

* g adsorbed/ g dry net weight of the adsorbent

Table 5.5: Uptakes and selectivities for duplicate runs at experimental condition #2

	1	2	Average	STDV	Coefficient of variation (%)
Water uptake*	18.81E-03	18.35E-03	18.58E-03	3.24E-04	1.74
Ethanol uptake*	17.42E-02	17.86E-02	17.64E-02	3.07E-03	1.74
water selectivity	2.06	1.90	1.98	1.13E-01	5.74
Ethanol selectivity	0.48	0.53	0.51	2.90E-02	5.74

* g adsorbed/g dry net weight of the adsorbent

Table 5.6: Uptakes and selectivities for duplicate runs at experimental condition #3

	1	2	Average	STDV	Coefficient of variation (%)
Water uptake*	2.02E-02	1.77E-02	1.89E-02	1.77E-03	9.33
Ethanol uptake*	1.97E-01	1.89E-01	1.93E-01	5.57E-03	2.90
water selectivity	1.93	1.83	1.88	7.30E-02	3.90
Ethanol selectivity	5.18E-01	5.47E-01	5.33E-01	2.07E-02	3.90

* g adsorbed/ g dry net weight of the adsorbent

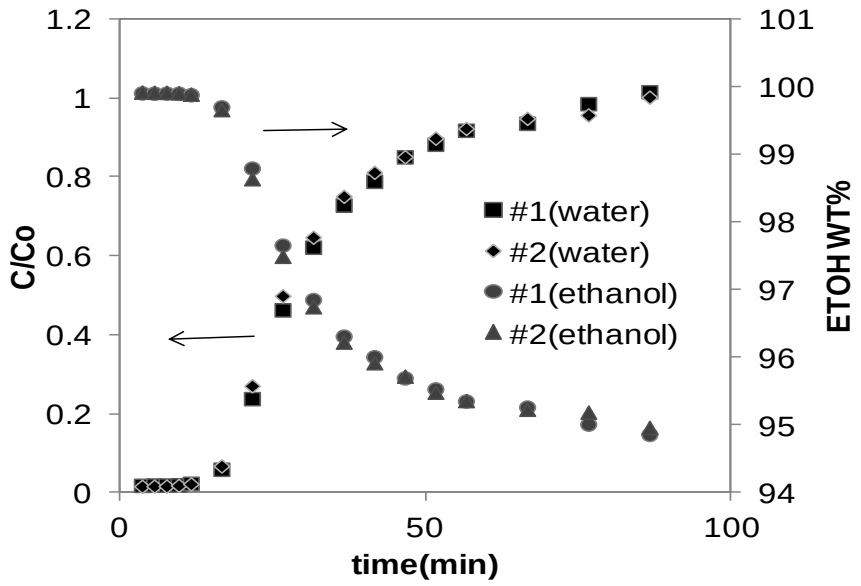

Figure 5.4: Ethanol and water breakthrough curves for duplicate runs at T= 95°C, P= 5 psig, ethanol feed concentration= 95 wt%, feed flow rate= 3 ml/min, particle size= 0.43- 1.18.

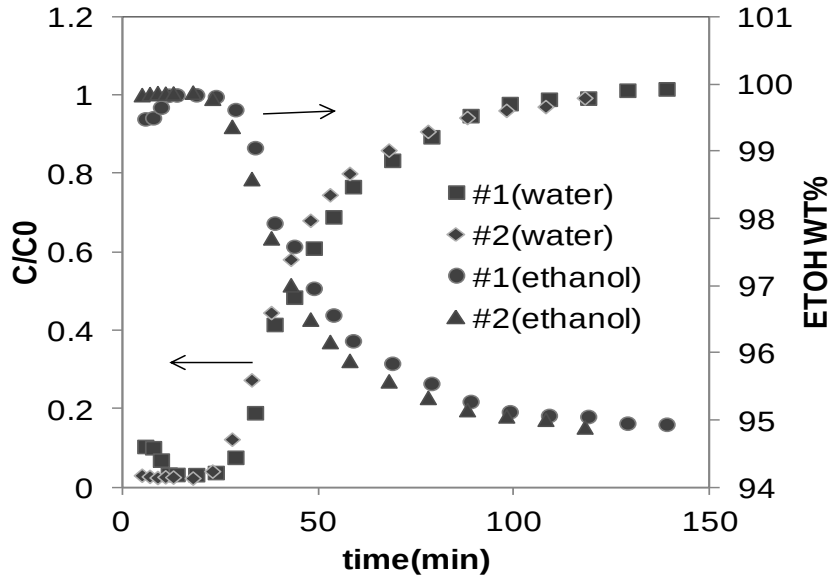

Figure 5.5: Ethanol and water breakthrough curves for duplicate runs at T= 95°C, P= 20.50 psig, Ethanol feed concentration= 95 wt%, feed flow rate= 3 ml/min, particle size= 0.43- 1.18.

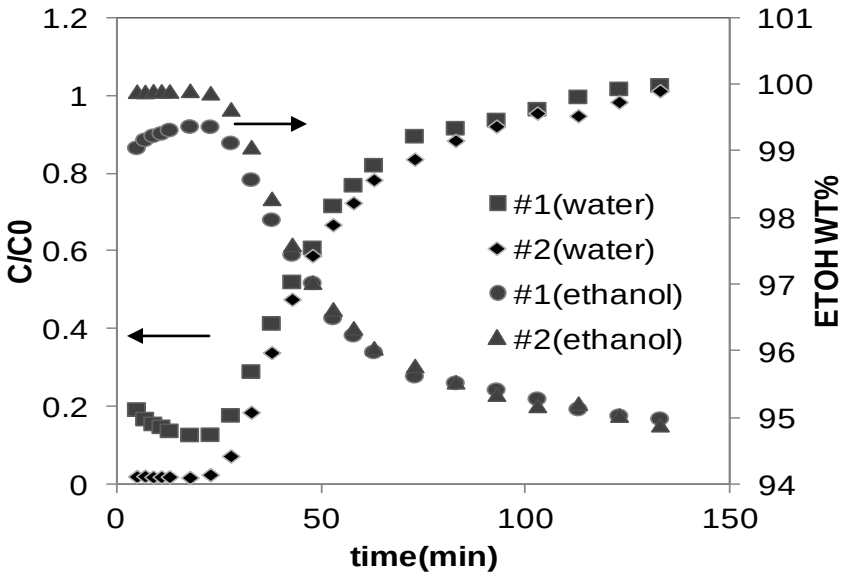

Figure 5.6: Ethanol and water breakthrough curves for duplicate runs at T= 90°C, P= 20.50 psig, Ethanol feed concentration= 95 wt%, feed flow rate= 3 ml/min, particle size= 0.43- 1.18.

Comparing the values of the coefficient of variation, it can be perceived that the adsorption system has a better reproducibility at lower pressure and higher temperature. Overall, with an average of 3.12% for the coefficient of variation, the adsorption system can be claimed to have a good reproducibility.

5.3 Dynamic Study

5.3.1 Effect of Temperature

To study the effects of temperature on the adsorption performance, experiments at ethanol vapor feed concentration of 95 wt %, pressure of 20.5 psig and feed flow rate of 3 ml/min at three different temperatures of 90°C, 95°C, and 110°C were carried out. The results are shown as breakthrough curves and temperature profiles in Figure 5.7 and 5.8.

As it can be seen from Figure 5.7- A, fuel grade ethanol (over 99 wt %) was achieved from lower ethanol concentration of 95 wt% at all three different temperatures. According to Figure 5.7- B, by increasing the bed temperature the breakthrough time decreases which could be related to the lower bed capacity at higher temperatures. Hu and Xie (2001), Wang et al. (2010) and Simo et al. (2009) also reported that the plateau length of the breakthrough curve decreased by increasing the temperature. The slope of the breakthrough curve, on the other hand, slightly increases by increasing the temperature. The steeper breakthrough curve infers the higher rate of adsorption which is caused by higher rate of diffusion of adsorbate molecules into the adsorbent pores resulting in inferior bed performance. Mainly there are three mass transfer resistances controlling the adsorbent uptake: external film resistance, macropore resistance and micropore resistance. The macropore and micropore resistances show strong temperature dependence while the external resistance shows only slight temperature dependence (Fogler, 2006). Since the mass transfer rate changes slightly by changing the temperature, as depicted in Figure 5.7- B, the

external mass transfer can be considered as the governing mass transfer mechanism. The calculated external mass transfer coefficients are 11.03E-03 m/s, 11.26E-03 m/s and 11.45E-03 m/s at temperatures 90°C, 95°C and 110°C, respectively. The external mass transfer coefficient values conform to the fact that the rate of mass transfer increases slightly by increasing the temperature. Simo et al. (2009) observed prominent temperature dependence in their Pressure Swing Adsorption (PSA) system using 3A° Zeolite, which was justified as domination of micropore diffusion mechanism.

From the temperature profiles in Figure 5.8, it can be observed that the temperature rose during the course of adsorption process and the extent of temperature rising increased by decreasing the temperature which implies more water adsorption at lower temperatures. The amount of water and ethanol adsorbed at equilibrium per unit weight of the adsorbent are shown in Figure 5.9. As it can be seen, at higher temperatures, less water and ethanol is adsorbed. However the rate of decrease in amount of ethanol adsorbed by increasing the temperature is faster than that of water which leads to higher separation factors at higher temperatures, as shown in Figure 5.10. Baylak et al. (2012) used raw canola meal as an adsorbent for ethanol dehydration at atmospheric pressure. They studied the effect of temperature at 75°C, 80°C, 85°C and 90°C and found that the best water uptake and selectivity was obtained at column temperature of 85°C.

The observed temperature rises, as shown in Figure 5.8, indicated both water and ethanol adsorption by protein extracted canola meal was exothermic adsorption.

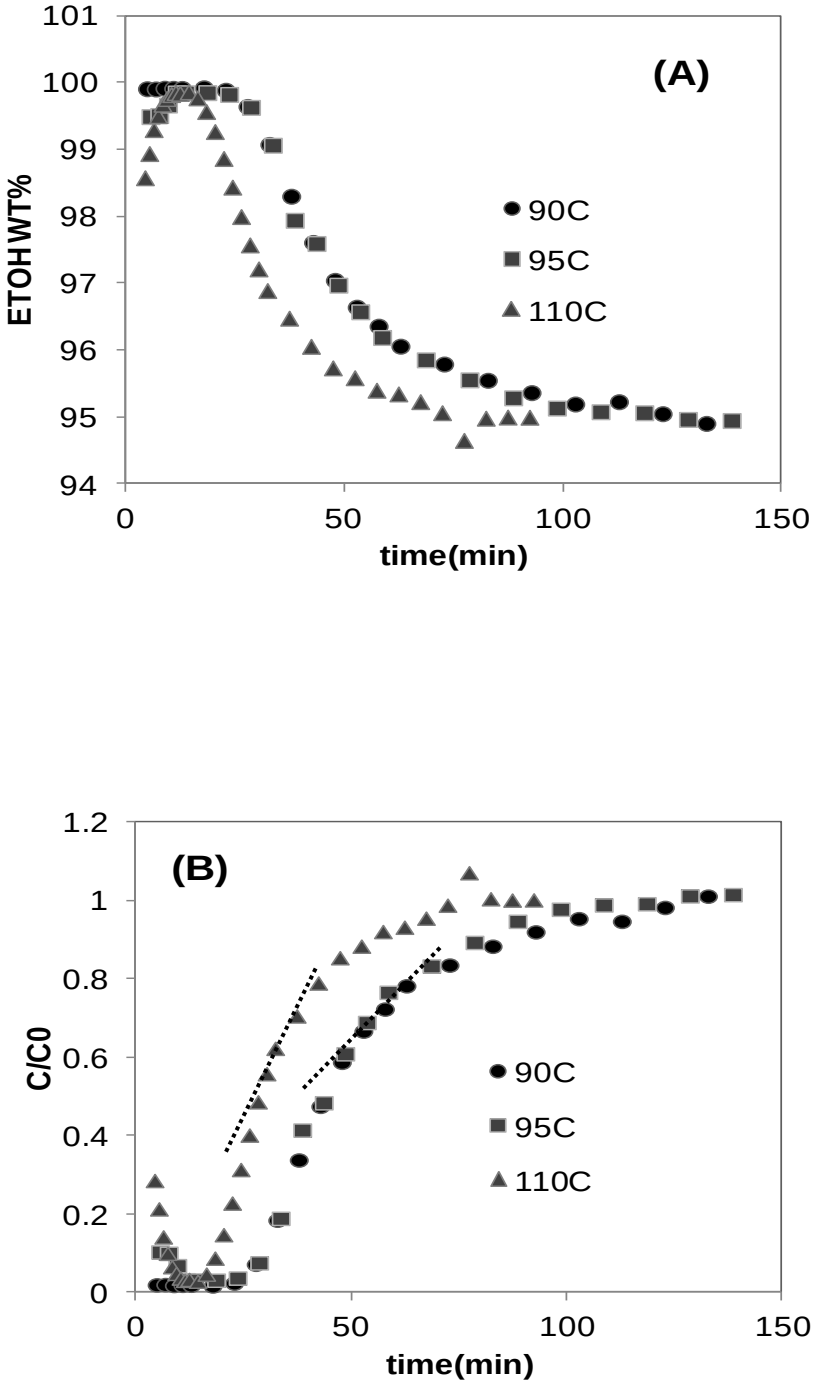

Figure 5.7: Breakthrough curves at different temperatures. (A) Ethanol concentration in the effluent (wt %) vs. time. (B) Dimensionless water concentration in the effluent C/C0 vs. time. All runs were at ethanol feed concentration of 95 wt% and pressure of 20.50 psig.

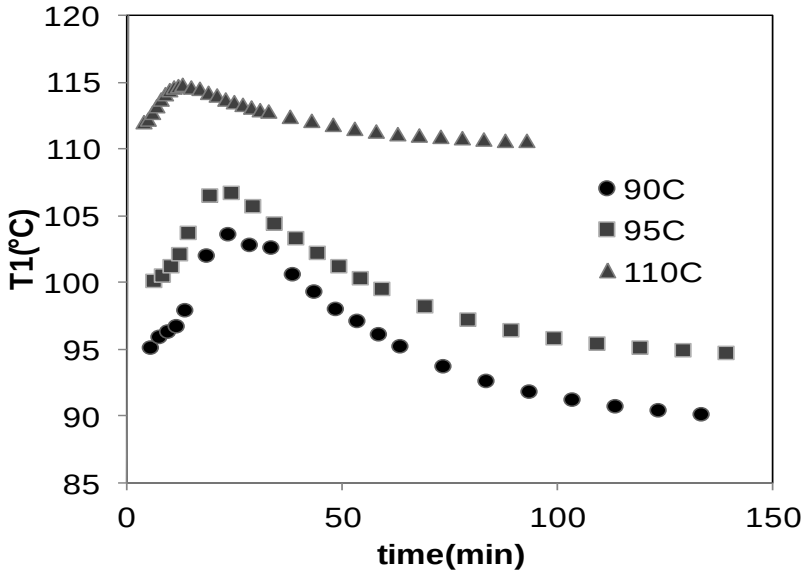

Figure 5.8: Temperature profiles at different temperatures. Experimental conditions: ethanol feed concentration of 95%, pressure of 20.50 psig. T1 corresponds to the temperature at the top of the column.

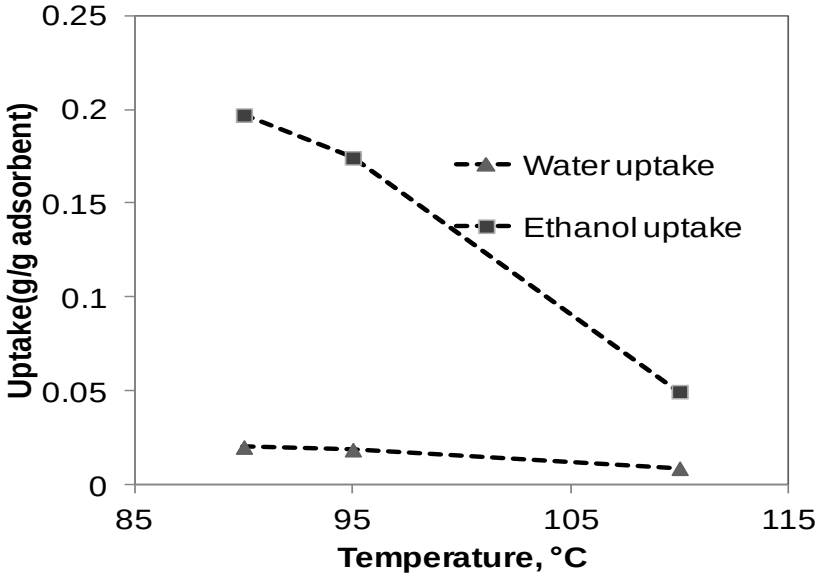

Figure 5.9: Water and ethanol uptakes at equilibrium at different temperatures.

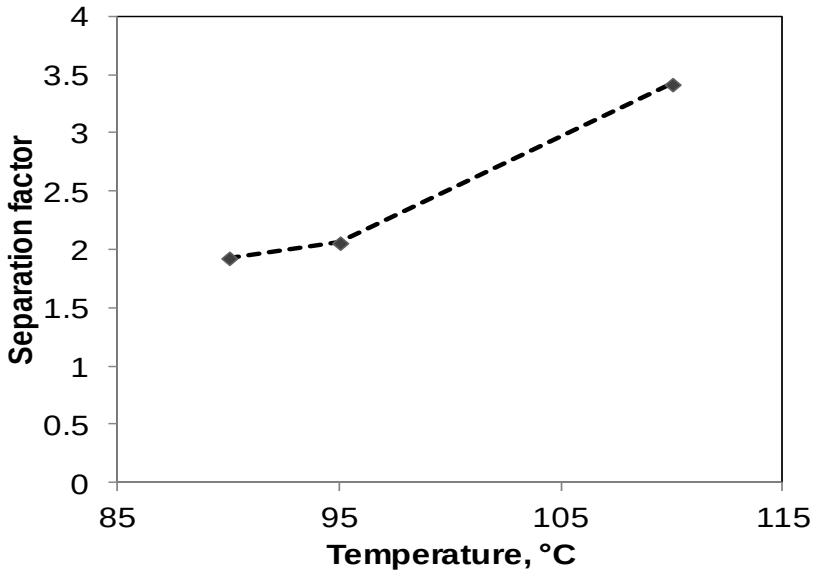

Figure 5.10: Effect of temperature on separation factor.

5.3.2 Effect of Vapor Feed Concentration

The effect of vapor feed concentration was investigated by maintaining the column temperature at 90°C, feed flow rate at 3 ml/min and pressure at 20.50 psig for three different ethanol feed concentrations of 85 wt%, 90 wt%, and 95 wt%. As indicated in Figure 5.11, the breakthrough time decreases by increasing the water feed concentration owing to the fact that when the feed water concentration is higher, more water is introduced to the adsorbent molecules; the driving force in the vapor phase is higher; as a result, the bed gets saturated faster. The observed breakthrough times were 17.38, 22.67 and 27.74 minutes for 15%, 10% and 5% water feed concentrations, respectively. These results conform to the results of Simo et al. (2009), Al-Asheh et al. (2004) and Benson and George (2005).

However, the rate of the mass transfer increases slightly by increasing the water feed concentration, as shown in Figure 5.11. As the bulk concentration increases, the film resistance

decreases leading to a higher mass transfer rate. The external mass transfer coefficients were determined to be 11.03E-03 m/s, 11.41E-03 m/s and 11.57E-03 m/s for ethanol feed concentrations of 95 wt%, 90 wt% and 85 wt%, respectively.

The separation factor increases as the water vapor feed concentration decrease, as shown in Figure 5.12. This can be elucidated by considering the effect of vapor feed concentration on the equilibrium loadings of water and ethanol. From Figures 5.13 and Figure 5.14, it can be seen that the extent of change in water uptake by decreasing the water feed concentration is more significant than that of ethanol which leads to higher separation factors for lower water feed concentrations.

Figure 5.13 shows equilibrium water loading versus relative humidity. It can be observed that by increasing the water vapor feed concentration the water equilibrium loading increases, which can be also observed in temperature profiles in Figure 5.15, showing higher temperature rises by increasing the water feed concentration. The observed temperature rises for ethanol feed concentrations of 95 wt%, 90 wt% and 85 wt% were 11.5°C, 16.4°C and 20.1°C, respectively. The more water is introduced to the bed, the more heat is generated causing a higher temperature rise.

In ethanol dehydration industry the adsorption process is terminated at breakthrough point, an arbitrary point in which the effluent no longer satisfies the objectives. Accordingly, the selectivity at breakthrough point is of particular importance. As it can be seen from Figure 5.16, the selectivity at breakthrough point increases by decreasing the water feed concentration. It can also be observed that selectivity at breakthrough point is higher than that at equilibrium which could be due to the higher temperature of the bed at breakthrough time.

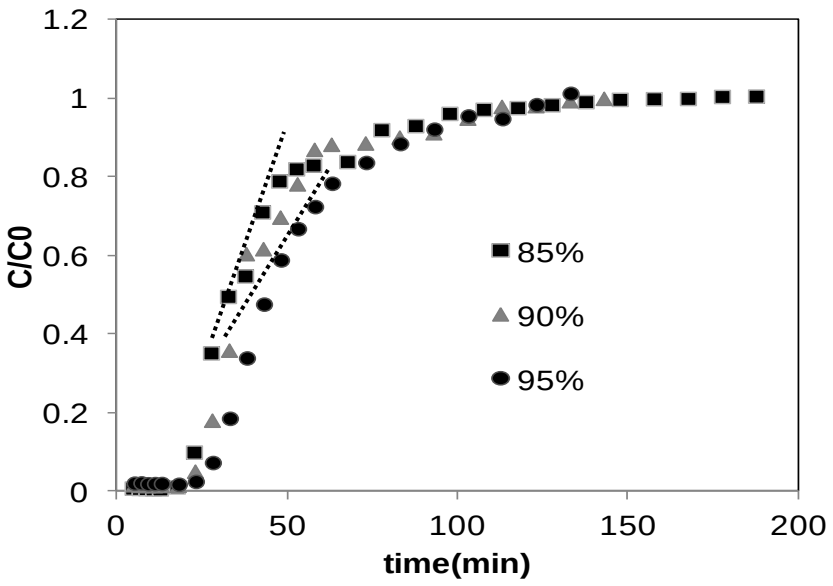

Figure 5.11: Breakthrough curve at different ethanol vapor feed concentration. All the runs were carried out at temperature of 90°C and pressure of 20.50 psig.

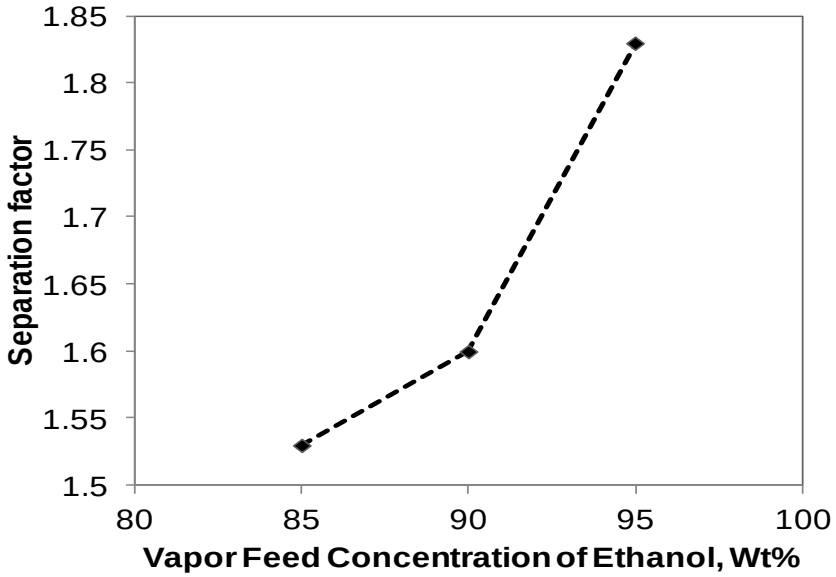

Figure 5.12: Effect of vapor feed concentration on separation factor.

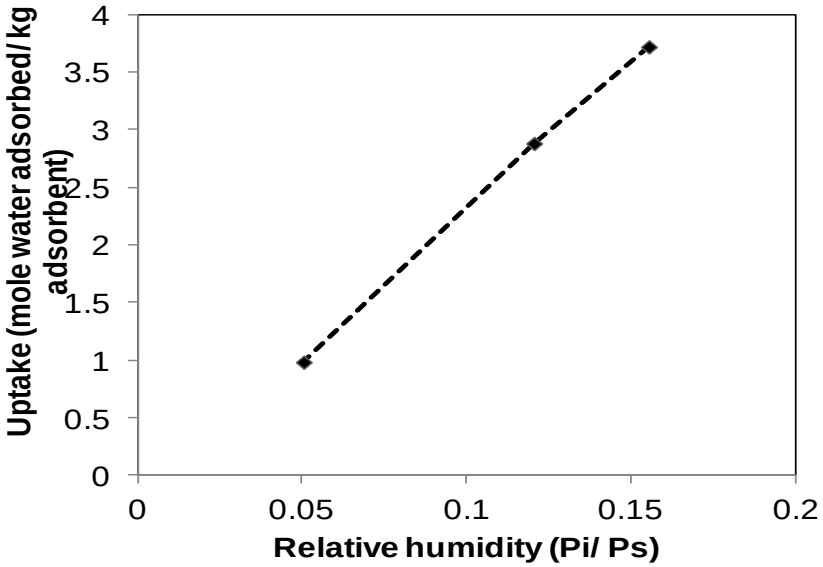

Figure 5.13: Variation of equilibrium water uptake by relative humidity.

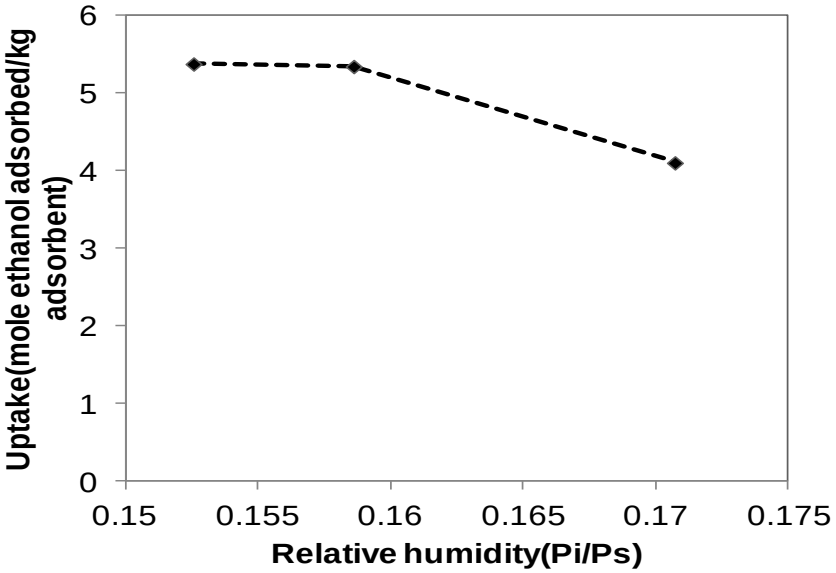

Figure 5.14: Variation of equilibrium ethanol uptake by relative humidity.

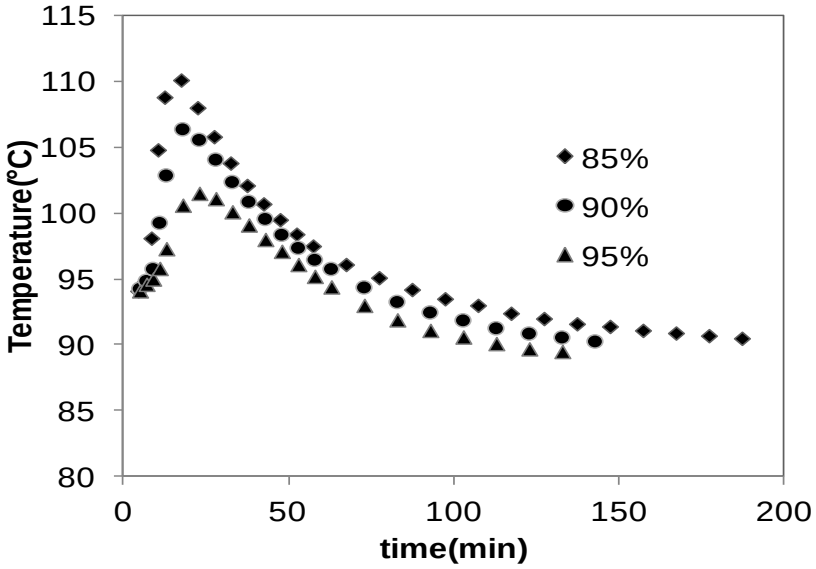

Figure 5.15: Temperature profiles at different feed concentrations.

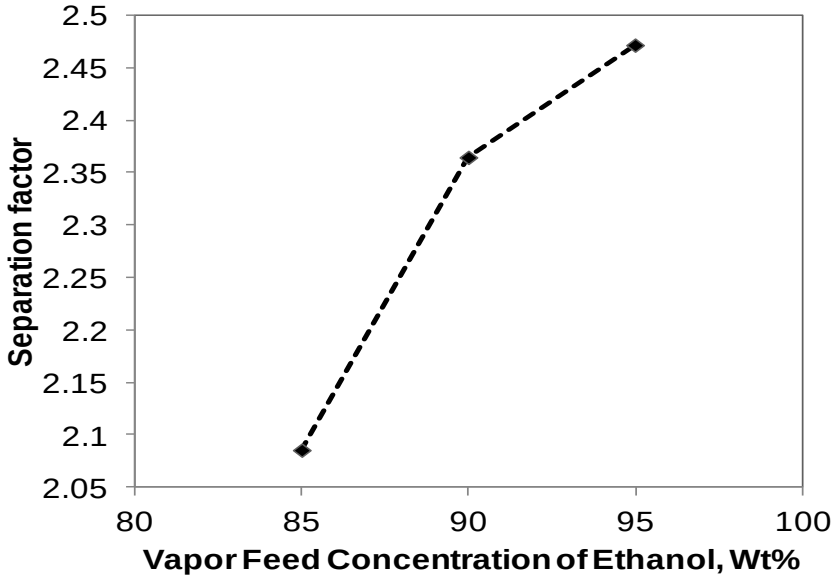

Figure 5.16: Effect of vapor feed concentration on separation factor.

5.3.3 Effect of Feed Flow rate

Two experiments were designed to study the effects of feed flow rate on the adsorption performance by keeping the temperature of the column at 95°C, the pressure at 20.50 psig and the feed concentration at 95 wt%. The feed flow rates were held at 3 ml/min and 6 ml/min.

Water and ethanol concentration profiles are shown in Figure 5.17. From Figure 5.17- A, it can be seen that higher concentrations of ethanol were achieved at a lower feed flow rate. It was observed that ethanol with concentration of 99.8 wt% was produced at 3 ml/min, while the highest concentration of ethanol attained at 6 ml/min was 99.4%. However, ethanol over 99 wt% (fuel grade ethanol) was produced at both flow rates studied. These results are similar to those reported by Wang et al. (2010) and Hu and Xie (2011).

The slope of the breakthrough curve, as shown in Figure 5.17- B, was slightly steeper for higher feed flow rate of 6 ml/min, which could be correlated to the existence of film mass transfer resistance. Among three rate limiting mechanisms including external laminar film, macropore and micropore diffusions, only the first one is dependent on the feed flow rate. At low flow rates, the film surrounding the adsorbent particles is thicker causing a longer time for adsorbate to diffuse toward the adsorbent surface; therefore, the rate of the mass transfer is slower. However, by increasing the flow rate, the mass transfer rate increases due to the decrease in the thickness of the boundary layer.

The water and ethanol loadings as well as separation factors at breakthrough and equilibrium are summarized in Table 5.7. The residence times were calculated to be 9.47 s and 8.42 s for flow rates of 3 ml/min and 6 ml/min, respectively, which explains the higher loadings at lower flow rate of 3 ml/min. The higher the flow rate, the shorter is the contact time between the adsorbate

and the adsorbent molecules leading to a lower uptake. The separation factor, on the other hand, increases by increasing the flow rate.

From Table 5.7, it can be elucidated that at breakthrough, water and ethanol uptakes decreased slightly by increasing the flow rate, which caused the separation factor to be almost the same whereas, at equilibrium, by increasing the flow rate the water uptake remained the same, but the ethanol uptake decreased significantly. As a result, the separation factor increased considerably.

The breakthrough time decreased from 27.84 to 12.20 minutes as the flow rate increased. This observation could be due to the shorter contact time at the higher flow rate, which caused the bed to reach its adsorption capacity earlier compared to that at the lower flow rate.

Table 5.7: Water/ ethanol uptakes at breakthrough time and equilibrium as well as separation factors for different feed flow rates.

Feed Flow Rate(ml/min)	Breakthrough			Equilibrium		
	Water uptake*	Ethanol uptake*	Separation factor	Water uptake	Ethanol uptake	Separation factor
3	8.20	61.10	2.48	18.30	178.60	1.89
6	6.70	50.30	2.49	18.20	140.70	2.42

*mg/g adsorbent

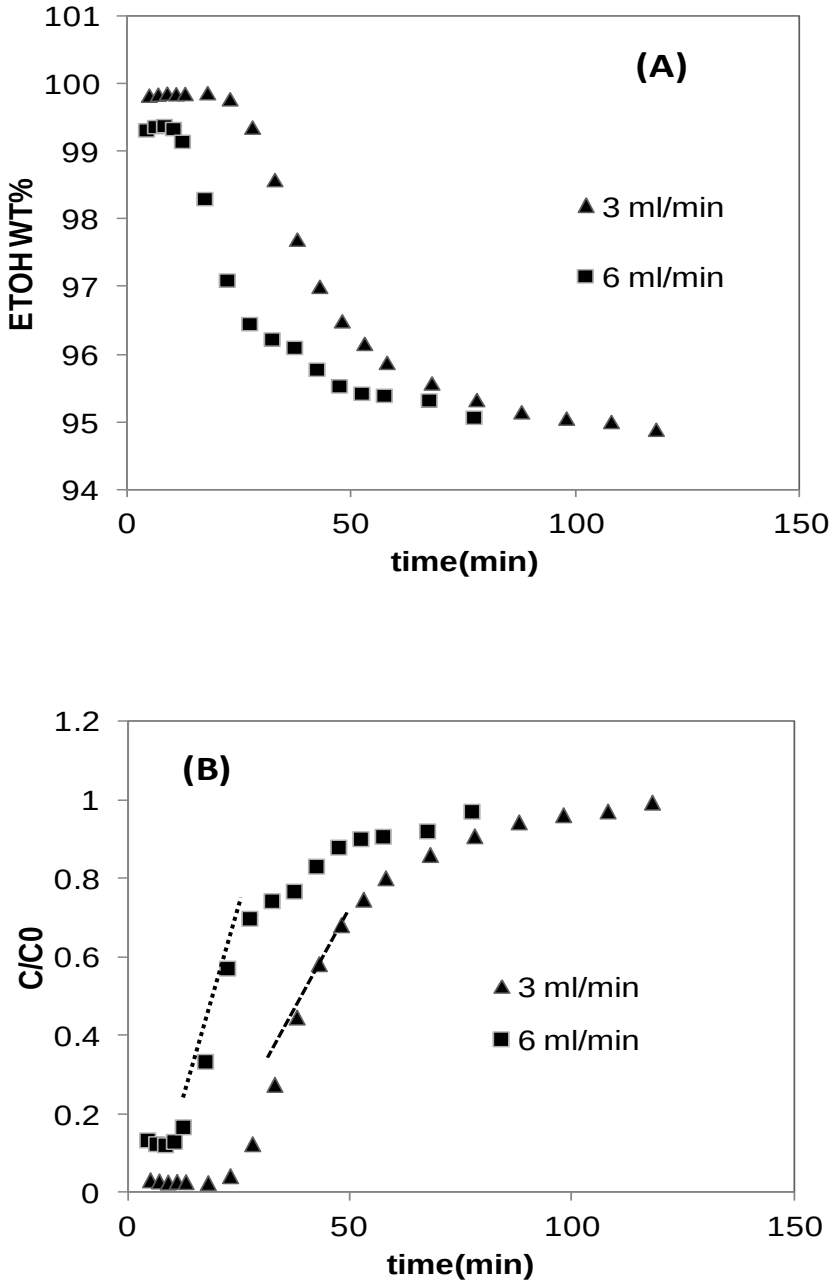

Figure 5.17: Breakthrough curves at different superficial velocities. (A) Ethanol concentration in the effluent (wt %) vs. time. (B) Dimensionless water concentration in the effluent C/C0 vs. time. Experimental conditions: temperature at 95°C, pressure at 20.50 psig, ethanol feed concentration at 95 wt%.

5.3.4 Effect of Particle size

The adsorbent particle size can have a major impact on the adsorption process. Surface area, voidage, pressure drop and film coefficient as well as intraparticle transport processes can all be affected by changing the adsorbent particle size (Hu and Xie, 2001; Simo et al., 2009).

To investigate how the change of the adsorbent particle size affects the adsorption process, two experiments were performed by holding the temperature at 95°C, pressure at 20.5 psig and the feed concentration at 95 wt% for two different particle sizes of 0.43-1.18 mm in the powder form and 5 mm in the pellet form. The concentration and temperature profiles are shown in Figure 5.18 and 5.19. It can be seen from Figure 5.18 that by reducing the particle size from 5 mm to 0.43-1.18 mm, the breakthrough time increases from 13.68 min to 27.84 min. Furthermore, a higher concentration of ethanol is produced for smaller particle sizes, as shown in Figure 5.18-B. Al- Asheh et al. (2004) observed similar results by comparing three different sizes of molecular sieves. They stated that the longer breakthrough time and the higher ethanol content produced using smaller particle sizes were due to adsorbent's higher surface area.

From Figure 5.18- A, it is evident that the slope of the breakthrough curve increases by decreasing the adsorbent particle size implying a higher mass transfer rate. This observation is in agreement with the estimated values of the external mass transfer coefficient. The calculated mass transfer coefficients are 11.26E-03 m/s and 8.99E-03 m/s for particles with diameter of 0.43- 1.18 mm and 5 mm, respectively. However, Simon et al. (2009) concluded that the aforementioned observations are mainly due to the presence of the macropore resistance which decreases by reducing the adsorbent particle size.

From the temperature profiles in Figure 5.19, it can be noticed that a sharper and narrower temperature profile with a higher temperature rise is attained for smaller particle sizes, which can be caused by a higher mass transfer rate.

The equilibrium loadings of water and ethanol along with selectivities are displayed in Table 5.8.

The water and ethanol loadings increase by decreasing the particle size due to the higher surface area of the smaller particles which provides more adsorption sites available to the adsorbate molecules. However, the selectivity did not change significantly as the particle size decreased which could be explained by the same extent of increase in water and ethanol uptakes. Anozie et al. (2010) used activated saw dust in five groups of particle sizes and reported that the adsorption capacity increased by decreasing the particle size.

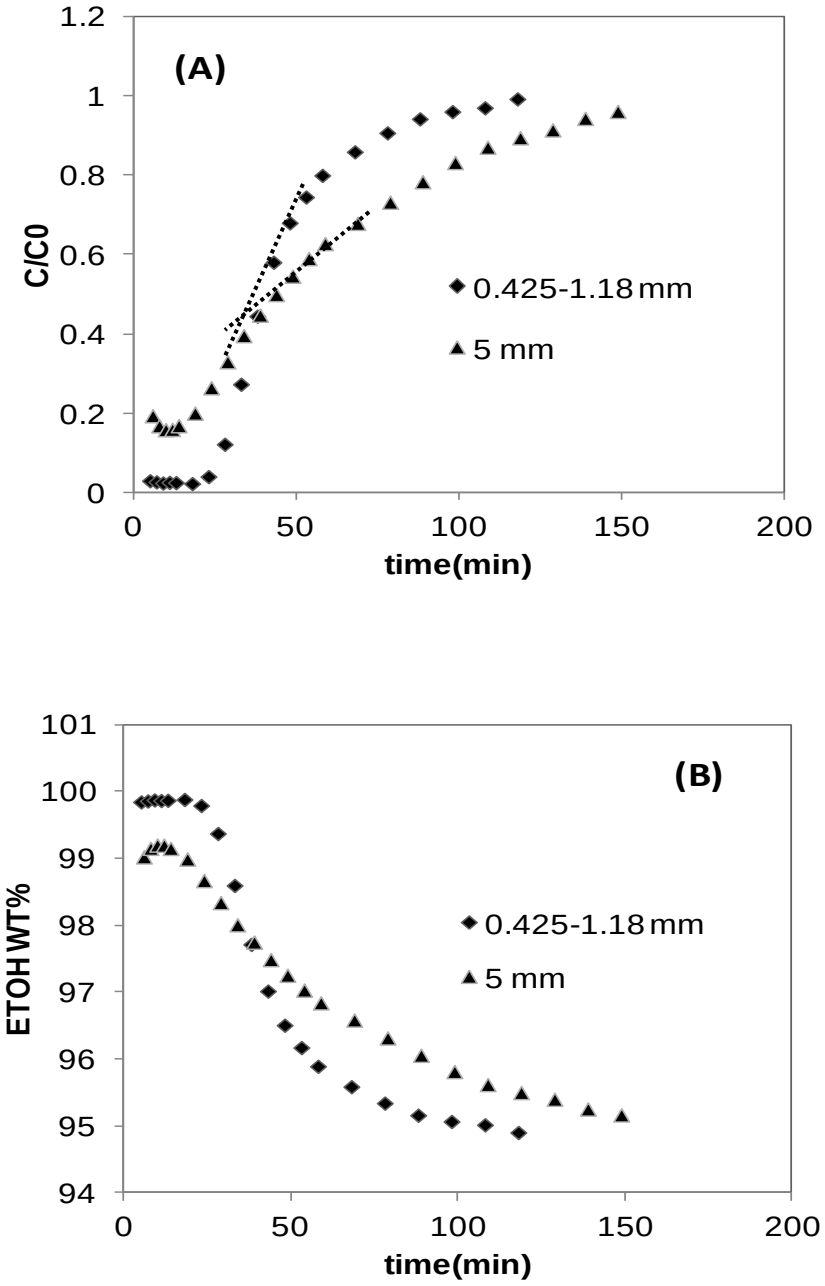

Figure 5.18: Breakthrough curves at different adsorbent particle sizes. (A) Ethanol concentration in the effluent (wt %) vs. time. (B) Dimensionless water concentration in the effluent C/C0 vs. time. Experimental conditions: temperature at 95°C, pressure at 20.50 psig, ethanol feed concentration at 95 wt%.

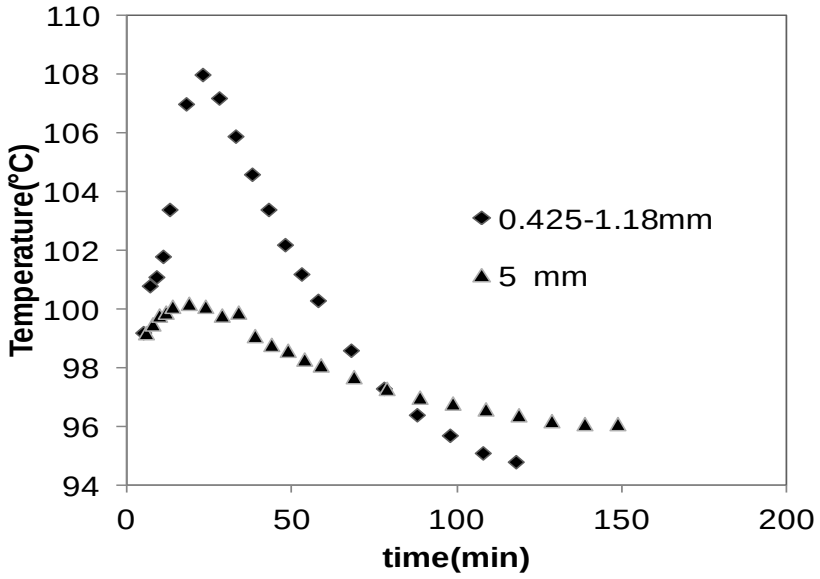

Figure 5.19: Variation of temperature with time for different adsorbent particle size.

Table 5.8: water/ ethanol loading at equilibrium as well as separation factors for different adsorbent particle sizes.

Particle size(mm)	Water equilibrium loading*	Ethanol equilibrium loading*	Selectivity of water to ethanol
0.43-1.18	1.80E-02	1.78E-01	18.97E-01
5	1.50E-02	1.49E-01	18.94E01

*g water/ g adsorbent

5.3.5 Effect of Pressure

There is not much information in the open literature on the effect of pressure in a Pressure Swing Adsorption (PSA) system using biosorbents. Therefore, two experiments were designed to examine the pressure effect in an adsorption process. The experiments were carried out for two different pressures of 20.5 psig and 5 psig at column temperature of 95°C, ethanol feed

concentration of 95 wt% and feed flow rate of 3 ml/min. The first pressure was chosen to be close to the industrial condition while the second pressure was selected close to the atmospheric pressure for comparison purposes.

The macropore resistance is the only mechanism that is dependent on the pressure. The macropore resistance consists of two diffusion mechanisms: Knudsen diffusion and molecular (bulk) diffusion.

Knudsen diffusion occurs when the pore diameter is smaller than the mean free path (λ), the average distance travelled by a molecule of gas between successive collisions. However, when the mean free path is smaller than the pore diameter, the molecular (bulk) diffusion is controlling the mass transfer rate.

The mean free path is inversely proportional to the pressure of the system; therefore, by decreasing the pressure the mean free path increases leading to a transition from bulk diffusion to Knudsen diffusion. The Knudsen diffusion coefficient is not a function of pressure (Simo et al., 2009). Consequently, if this mechanism is the governing mechanism, changing the pressure of the system should not result in any change in the breakthrough curves. However, as it can be noted from Figure 5.20, the slope of the breakthrough curve increases by decreasing the pressure implying that the molecular (bulk) diffusion is the controlling mechanism.

Table 5.9 summarizes the water and ethanol loadings at breakthrough and equilibrium conditions as well as selectivities. It can be seen that, as the pressure decreases the water and ethanol loadings at breakthrough and equilibrium decrease owing to the decrease in driving force, while the selectivity of water to ethanol increases due to the different extent of decrease in water and ethanol loadings.

Table 5.9: Water and ethanol loadings and separation factors at equilibrium and breakthrough point for different pressures.

Pressure(Psig)		Equilibrium Uptake*	Breakthrough Uptake*	Equilibrium Selectivity	Breakthrough Selectivity
20.50	Water	1.88E-02	9.30E-03	2.05	3.29
5		1.13E-02	4.80E-03	2.43	3.47
20.50	Ethanol	1.74E-01	5.41E-02	0.48	0.30
5		8.77E-02	2.60E-02	0.41	0.29

*g/ g adsorbent

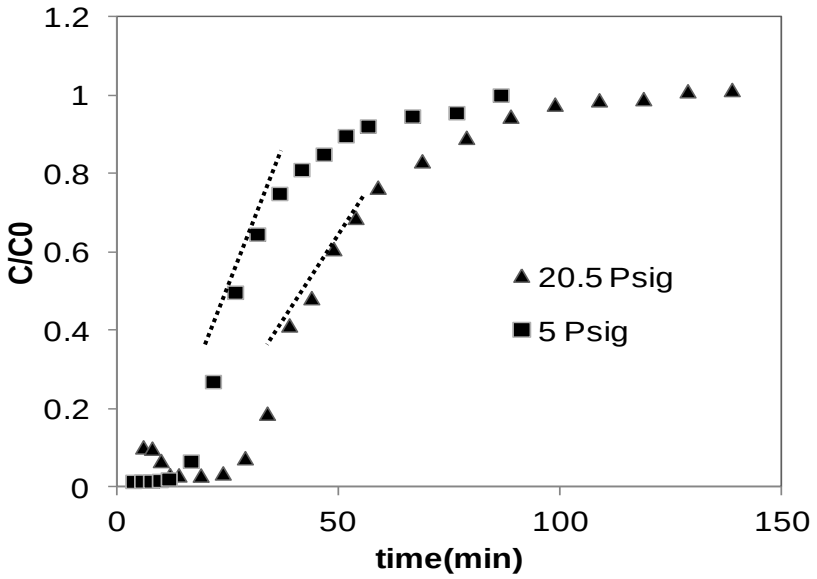

Figure 5.20: Breakthrough curves at different pressures. All the runs were performed at temperature of 95°C and ethanol feed concentration of 95 w%.

5.4 Regeneration and Adsorbent Stability

Pressure swing adsorption process comprises two successive steps: high pressure adsorption followed by low pressure regeneration. In order to have an efficient adsorption process, it is essential to make sure that the bed has been regenerated sufficiently.

The partial pressure of the adsorbed components can be reduced by lowering the total pressure of the bed or by passing an inert gas in a reverse direction to that of adsorption while the total pressure is kept constant. However, a combination of the two methods can be used as well (Thomas and Crittenden, 1998). Passing the inert gas in a same direction of adsorption leads to the readsorption of water molecules carried out from more to less saturated part of the bed during the regeneration process. Moreover, the adsorption heat stored in the bed is not employed properly.

To study the regeneration process, experiments were carried out at temperature of 90°C, feed concentration of 80 wt% and feed flow rate of 3 ml/min. The total pressure of the system during the adsorption process was kept constant at 20.50 psig. For the regeneration process, the pressure was lowered to (-10) psig. Nitrogen, 1.22 L/min was provided from the bottom of the column as a purging agent for 4 hours. After regeneration, the column was run for adsorption again at the same condition as that for the previous run.

Temperature profiles for the regeneration process at the top and bottom of the column are depicted in Figure 5.21. As it can be seen the temperature starts decreasing at the beginning of desorption process owing to the fact that desorption is an endothermic process then it begins rising until the initial temperature profiles are obtained. Simo et al. (2009) also reported the same

trend in temperature profiles for regeneration of type 3A molecular sieves in an adsorption process for ethanol dehydration.

The rate of desorption declines as the process proceeds due to the decrease in the water concentration.

In order to see whether the in situ regeneration was sufficient or not, the adsorption cycles were compared. As it can be seen from Figures 5.22 and 5.23, the temperature and concentration profiles are homologous implying the fact that the bed was fully dried after the online regeneration. However, to further confirm these observations, the adsorbent was removed from the bed after the second experiment and was weighted. The initial dry net weight and the adsorbent weight after regeneration were 402.50 g and 400.21 g showing less than 0.60 % difference. The difference may be because of the trace amount of canola meal attached to the wall inside of the column.

Stability of the adsorbent was evaluated in packing the protein extracted canola meal in the fixed bed column for cycles of ethanol dehydration and regeneration. Each adsorption process was followed by regeneration using nitrogen gas as a purging agent. Over 35 cycles of adsorption/desorption were carried out during two months. Performance of canola meal for ethanol dehydration remains constant. The canola meal adsorbent has been used without deterioration. Because the process deals with ethanol and water saturation column was dried at 90°C right after the dehydration, microbes are not able to grow effectively on the protein extracted canola meal. Thus the significant decomposition of canola meal material by microbes is not observed. This infers that the protein extracted canola meal is a stable adsorbent for this application.

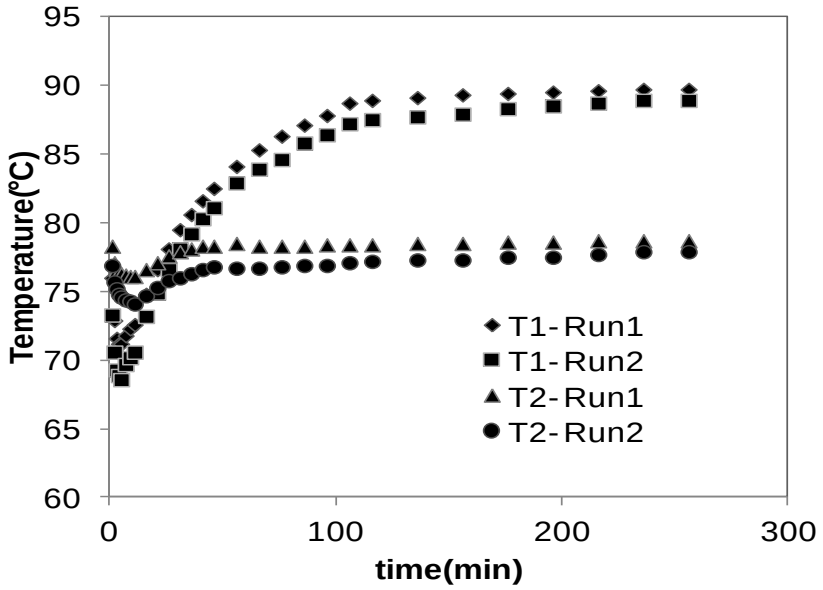

Figure 5.21: Variation of temperature with time for regeneration process. T1 corresponds to the temperature of the column at the top and T2 corresponds to the temperature of the column at the bottom. Experiments were conducted at pressure of 0.30 bars and nitrogen flow rate of 1.22 L/min for 4 hours.

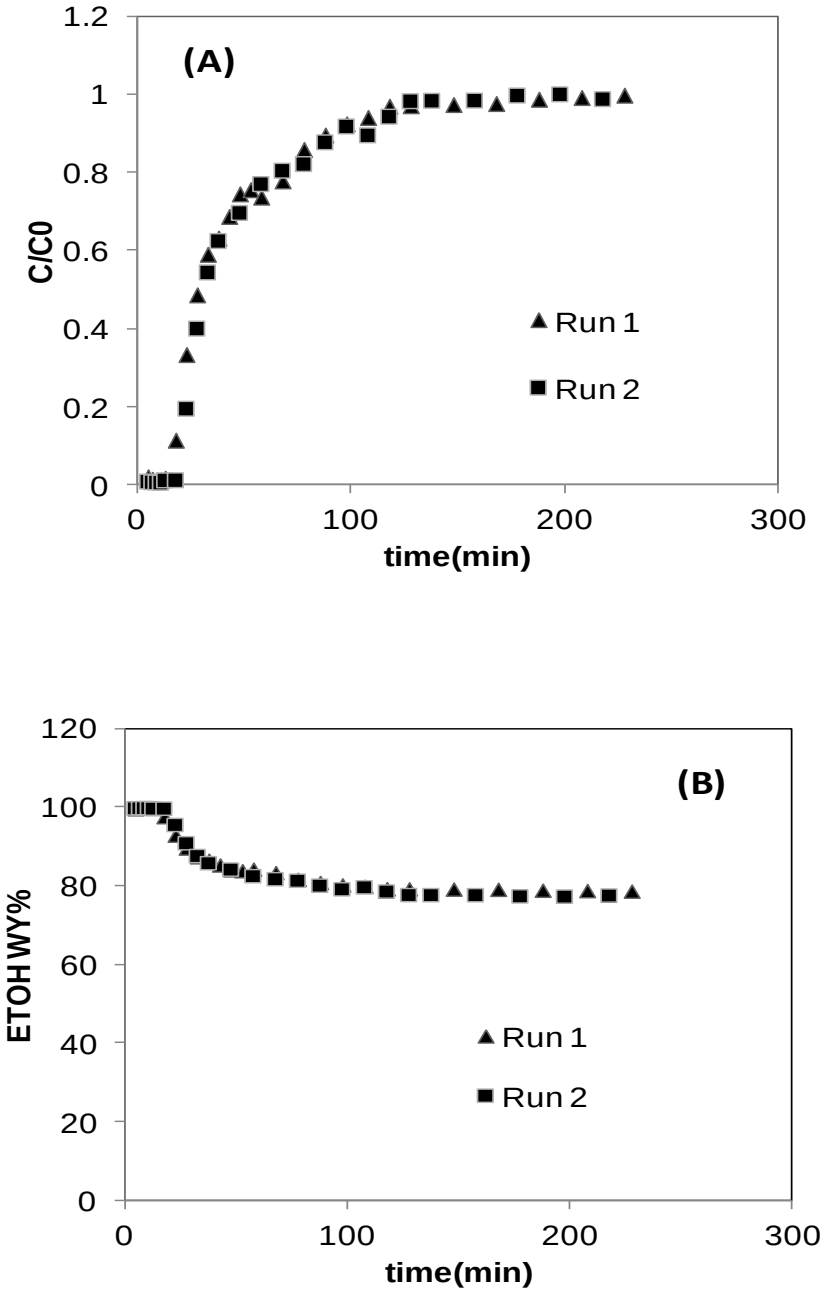

Figure 5.22: Breakthrough curves for adsorption processes. (A) Ethanol concentration in the effluent (wt %) vs. time. (B) Dimensionless water concentration in the effluent C/C0 vs. time. Experimental conditions: temperature at 90°C, pressure at 20.50 psig and ethanol feed concentration at 80 wt%.

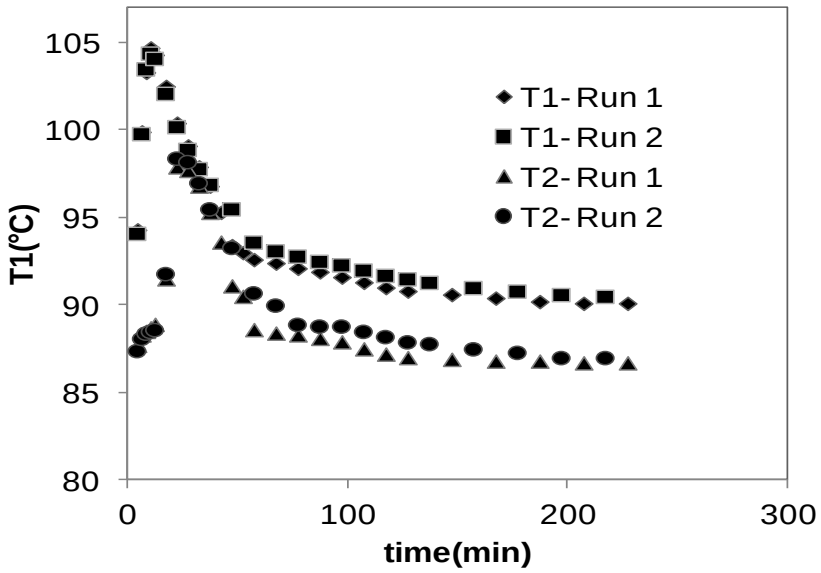

Figure 5.23: Variation of temperature with time during the course of adsorption. T1 and T2 correspond to the temperature of the column at the top and bottom, respectively.

5.5 Equilibrium Study

Adsorption equilibrium data were attained by utilizing the breakthrough curves. The equilibrium capacity of the adsorbent on uptake of water was assessed using the overall mass balance.

The water equilibrium uptakes were obtained at temperatures 90°C, 95°C and 110°C for the water feed concentrations in the range of 5 wt%- 35wt%. The pressure of the system was maintained at 20.50 Psig, and the feed flow rate was held at 3 ml/min. The adsorbent particle size was 0.43-1.18 mm.

There are several isotherm models that can represent an adsorption system. However, adsorption potential theory has been found to give the most reasonable representation of the equilibrium isotherm data in this study.

Adsorption Potential Theory

Adsorption potential theory is based on adsorption potential which is defined as the required work to convey adsorbate molecules from the gas phase to the adsorption sites. In this theory, unlike other adsorption isotherm models, equilibrium loadings at different temperatures are all presented in one curve known as the characteristic curve. The adsorption potential in the gas phase can be defined as (Chang et al., 2006c):

$$\varepsilon = RT\ln(P^s/P_i) \tag{5.1}$$

The function form of the potential theory, known as Dubinin- Polanyi theory, for microporous and large pore materials is described in Eq. (5.2) and Eq. (5.3), respectively.

$$lnq = lnq_0 - \frac{K_1}{\beta}\left[RTln\left(\frac{P^s}{P_i}\right)\right]^2 \tag{5.2}$$

$$lnq = lnq_0 - \frac{K_2}{\beta}\left[RTln\left(\frac{P^s}{P_i}\right)\right] \tag{5.3}$$

Where q= mass adsorbed per unit mass of adsorbent

q_0= limiting mass for adsorption

k_1, k_2= pore constant for micropore and large pore materials

ß= affinity coefficient

P_i, = Partial pressure of the adsorbate

P^s= saturated vapor pressure of the adsorbate

By plotting the equilibrium water uptake as a function of adsorption potential, shown in Figure 5.24, it can be noted that all the experimental data can be represented in one characteristic curve.

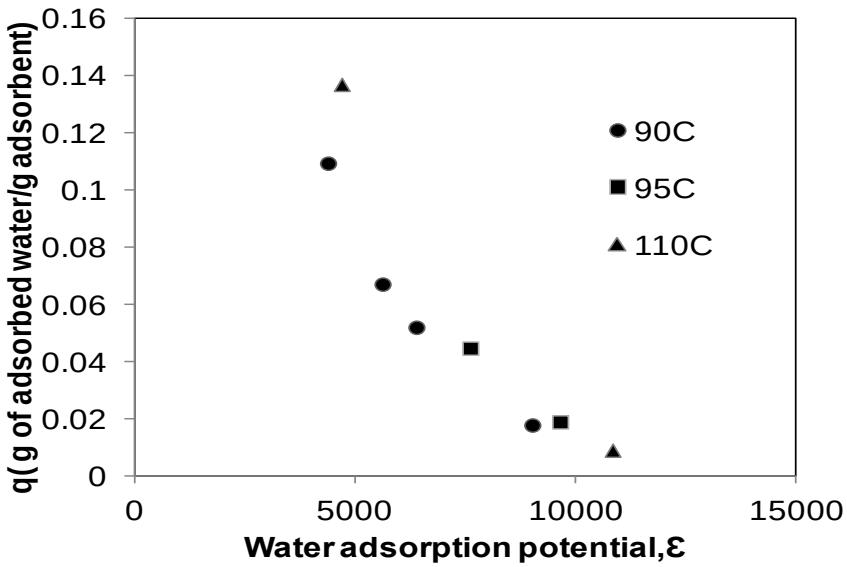

Figure 5.24: Characteristic curve for Polanyi adsorption potential theory.

Figure 5.25 and Figure 5.26 are the plots of equilibrium water uptake as a function of water adsorption potential according to Eq. (5.2) and Eq. (5.3), respectively.

Table 5.10 summarizes the constants for the Dubinin- Polanyi model for the micropore and large pore materials. As it can be seen, Eq. (5.3) which is representative for large pore or nonporous materials gave a better fit compared to Eq. (5.2).

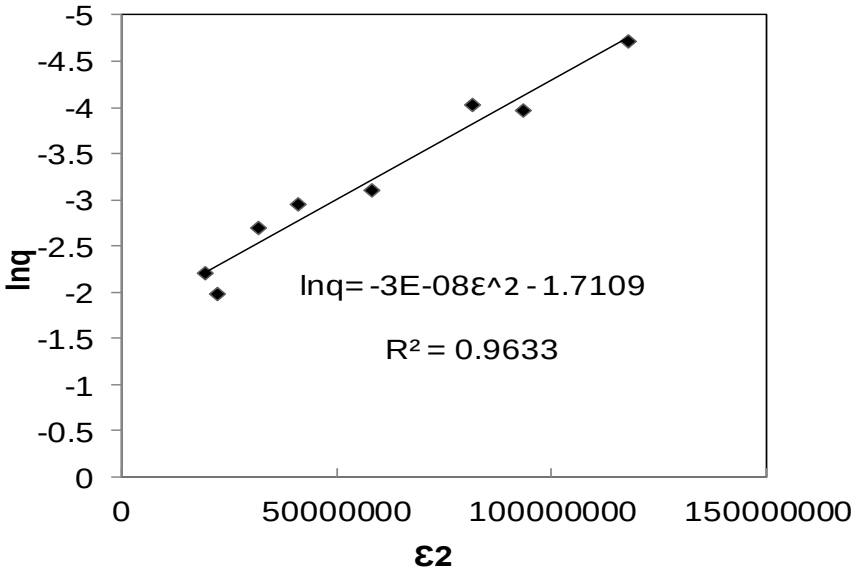

Figure 5.25: Dubinin- Polanyi model for microporous materials (● experimental data; - predicted by the model)

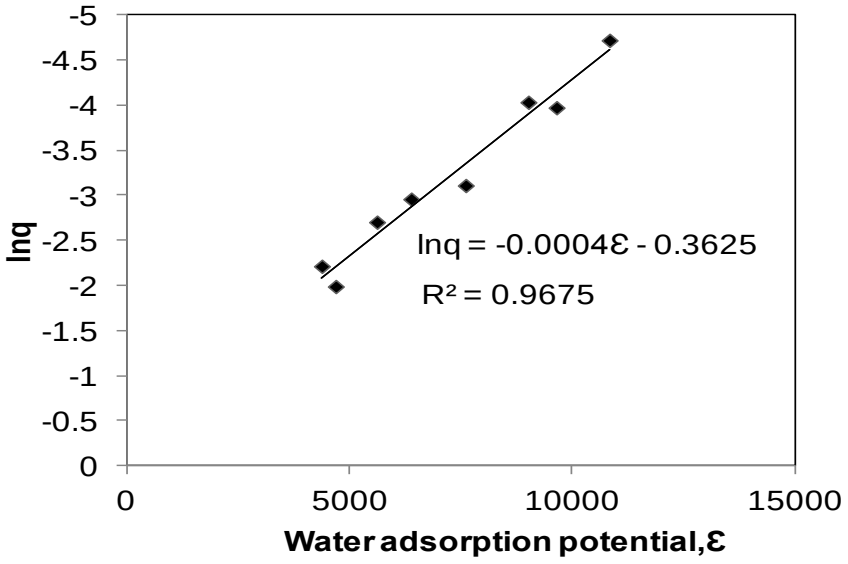

Figure 5.26: Dubinin- Polanyi model for large pore materials (● experimental data; - predicted by the model)

The equation for the straight line in Figure 5.26 is:

$$\ln q = -0.0004\,\varepsilon - 0.3625 \quad (5.4)$$

According to Eq. (5.3), the values for the limiting mass for the adsorption (q_0) and the coefficient $\Delta = k_2 / ß$ are estimated from the intercept and slope of the Eq. (5.4) to be 69.59% and 4E-04, respectively. Chang et al. (2006) reported these values as 16.33% and 3.28E-04 in an ethanol-water binary vapor system using cornmeal as the adsorbent.

The mean free energy of adsorption was evaluated using the following equation:

$$E = \frac{1}{\sqrt{2\Delta}} \quad (5.5)$$

The value of the mean free energy is an indication of the nature of the adsorption process. For the values of E between 8- 16 kJ /mol, the adsorption process is considered to be chemisorption while the process is physisorption for the values of E lower than 8 kJ/ mol (Dang et al., 2009). As it can be noted from Table 5.10, the value for the mean free energy is 0.04 kJ /mol, which infers the physical nature of the adsorption process in this study. Dang et al. (2009) used wheat straw to adsorb cadmium (II) and copper (II) ions in an aqueous system. They have estimated the value of mean free energy as 11.20 kJ /mol and 12.90 kJ /mol for Cd^{2+} and Cu^{2+}, respectively.

The major advantage of the adsorption potential theory compared to the other adsorption isotherm models is that only a limited number of data points are required to obtain the characteristic curve (Chang et al., 2006c)

Table 5.10: Constants for the Dubinin- Polanyi model for the micropore and large pore materials.

	q_0 (g/g adsorbent)	**Δ=k/ß**	**E=1/√2Δ(KJ/mol)**	**Correlation Coeff. R^2**	**Relative Error (%)**
Microporous	0.18	3E-08	4.17	0.96	7.00
Large Pore	0.69	4 E-04	0.04	0.97	4.70
Cornmeal(Chang et al., 2006)	0.16	3 E-04	0.04	0.96	____

In an adsorption system, thermodynamic parameters including the heat of adsorption (ΔH°), which are affected by the changes of the temperature, are sources of valuable information about the adsorption process. A negative value for the heat of adsorption infers the exothermic nature of the process (Farooq et al., 2010). It also helps to determine if the adsorption process is physisorption (physical adsorption) or chemisorption (chemical adsorption). If the value for the heat of adsorption is in the range of 20- 80 KJ/mol, the adsorption process is physical. However, a higher value in the range of 80- 400 kJ/mol is expected for a chemical adsorption process (Chowdhury et al., 2011).

The heat of adsorption is calculated according to Van't Hoff's equation (Fogler, 2006):

$$\frac{d(lnK_T)}{d(\frac{1}{T})} = -\frac{\Delta H^\circ}{R} \qquad (5.6)$$

Where $\Delta H°$ is enthalpy of the adsorption (kJ/mol). T is temperature in Kelvin, R is universal gas constant and K_T is the equilibrium thermodynamic constant. Values of K_T were determined by plotting ln (q_e/C_e) versus C_e and extrapolating to zero C_e (Khan and Singh, 1987).

The heat of adsorption was estimated to be - 35.81 kJ/ mol in this study which implies the physical and exothermic nature of the adsorption process.

5.6 Comparison

To study the usability of canola meal after protein extraction for ethanol dehydration, the adsorption performance of the biosorbent was compared to that of canola meal before protein extraction, other biosorbents and molecular sieves which are currently being used in the ethanol dehydration industry.

The effect of protein extraction was studied by comparing the adsorption performance of canola meal before and after protein extraction by conducting experiments at temperature of 110°C, pressure of 20.50 psig and ethanol feed concentrations of 80 and 65 wt%. Results, as shown in Table 5.11, demonstrated that canola meal residues after protein extraction was still able to selectively remove water from ethanol with slightly higher water and lower ethanol uptake than that of raw canola meal. The higher water uptake of canola meal after protein extraction could be due to the removal of nonpolar amino acid groups of protein content which show poor solubility in water.

Table 5.11: Comparison between canola meal before and after protein extraction.

	80 wt% ethanol			65 wt% ethanol		
	Water uptake*	Ethanol uptake*	SP**	Water uptake	Ethanol uptake	SP
Raw CM	4.40E-02	1.31E-01	1.34	0.09	0.11	1.53
PE- CM	8.27E-02	7.41E-02	2.78	0.14	0.08	3.42

*g adsorbed/g adsorbent; ** separation factor

Canola meal after protein extraction also exhibited comparable results to other biomaterials in terms of equilibrium water loading, as shown in Table 5.12.

Table 5.12: Comparison between protein extracted canola meal and other biosorbents.

Biomaterial	Equilibrium water loading (g/g adsorbent)*
Protein extracted canola meal	1.60E-02
Corn meal (Chang et al., 2006)	3.05E-02
Cassava pearls (Kim et al., 2011)	2.60E-02
Maize starch (Crawshaw and Hills, 1989)	2.30E-02
Oak chips (Benson and George, 2005)	2.20E-02
Kenaf core (Benson and George, 2005)	6.30E-03
Bleached wood pulp(Benson and George, 2005)	1.16E-02

*All the experiments were carried out at temperature range of 80- 100 °C and ethanol feed concentration of about ≈ 95 wt%.

It was shown it this study that protein extracted canola meal adsorbed a considerable amount of ethanol along with water. However, the biomaterial was proven to have a stable structure.

Therefore, a combination of this material with other biomaterials might result in higher selectivities of water over ethanol to enhance the adsorption performance of the biosorbent.

To compare the biosorbent with molecular sieves, two experiments were designed using the selected adsorbents in the form of pellets with diameter of 4-5 mm. The temperature and pressure of the system were held at 95 °C and 20.50 psig, respectively.

Table 5.13 presents a brief comparison in terms of uptake for water and ethanol as well as the selectivities at equilibrium.

Table 5.13: Comparison between protein extracted canola meal and molecular sieves.

	Water uptake ***	Ethanol uptake ***	Water Selectivity
PE- CM*	1.5E-02	1.49E-01	1.89
MS**	0.08	0.02	77.97

* Protein extracted canola meal; **Molecular sieves; ***g adsorbed/g adsorbent

As it can be seen from Table 5.13, a significant amount of ethanol was adsorbed along with water by canola meal compared to molecular sieves, which resulted in considerably lower values of water selectivity over ethanol for this biosorbent.

The water and ethanol breakthrough curves for the two experiments are shown in Figure 5.27. The breakthrough times were found to be 13.68 min and 518.03 min for protein extracted canola meal and molecular sieves, respectively. The longer breakthrough time for molecular sieves indicates the higher adsorption capacity of these materials compared to that of protein extracted canola meal. However, protein extracted canola meal is a biodegradable adsorbent which can be used in a fermentation plant for ethanol production after losing its adsorption capacity whereas molecular sieves are expensive adsorbents which cannot be used after saturated with water.

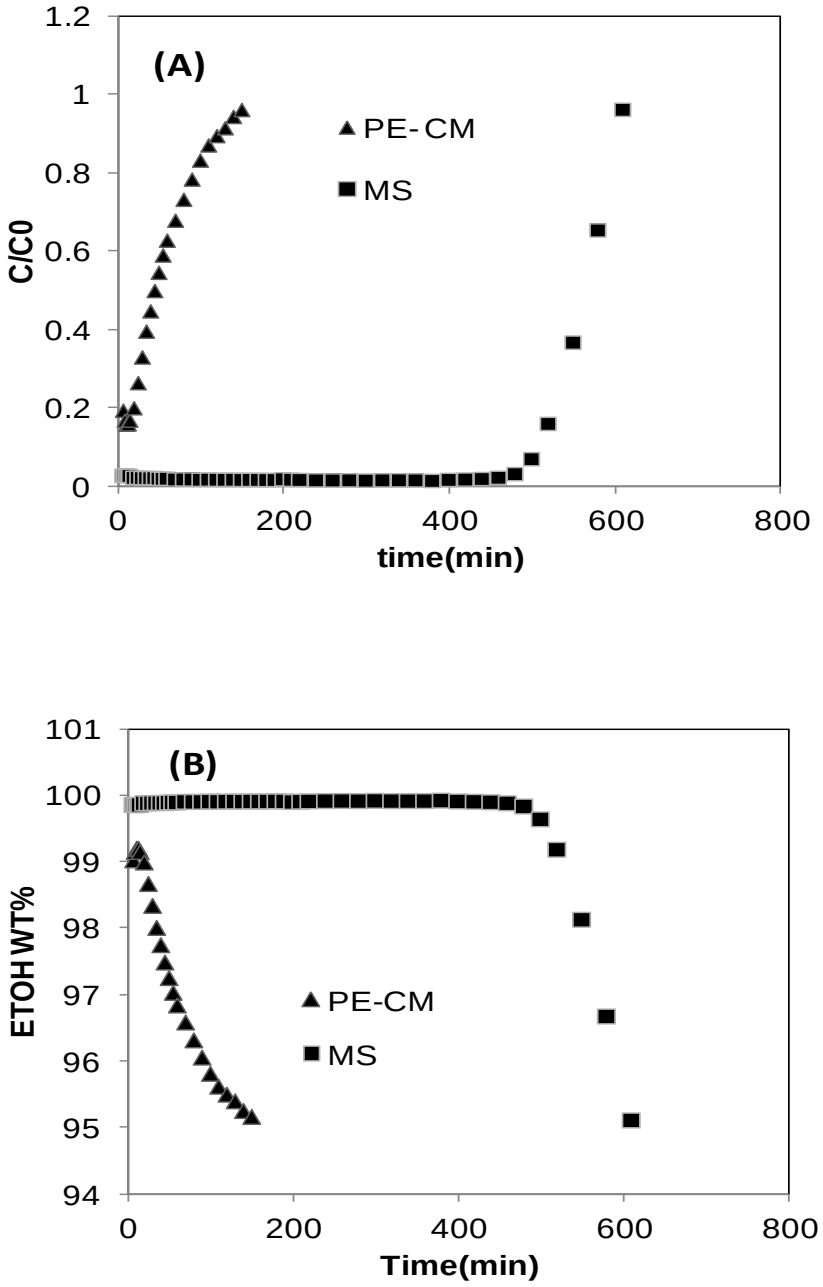

Figure 5.27: Breakthrough curves for two selected adsorbents (A) Dimensionless water concentration in the effluent C/C0 vs. time (B) Ethanol concentration in the effluent (wt %) vs. time. Experimental conditions: temperature at 95°C, pressure at 20.50 psig, ethanol feed concentration at 95 wt%.

6 Conclusions and Recommendations

6.1 Conclusions

The adsorption capability of canola meal after protein extraction for ethanol dehydration was investigated in a bench- scale pressure swing adsorption system. The equilibrium and kinetic studies of the process were carried out through breakthrough experiments. It was found that protein extracted canola meal had the capability to purify a 65- 95 wt% ethanol- water mixture to fuel grade ethanol (over 99 wt%).

The effects of operating conditions including temperature, pressure, feed flow rate and vapor feed concentration, as well as adsorbent particle size on the adsorption performance were examined. The results were evaluated in terms of adsorbent selectivity for water uptake, external mass transfer coefficient and breakthrough time. The calculated external mass transfer coefficients were in the range of 14.68- 23.27 m/s. From the experimental results, it can be concluded that higher mass transfer rate and selectivity of water over ethanol were observed at higher bed temperatures and at lower pressures. It was also observed that the selectivity of adsorbent to adsorb water over ethanol decreased when the water feed concentration increased. The breakthrough time decreased by increasing the temperature, water vapor feed concentration and the adsorbent particle size.

The equilibrium study was conducted using the breakthrough curves. It was found that the Dubinin- Polanyi model for large pore materials which is based on the adsorption potential theory gave the best fit to the experimental results. The parameters of the Dubinin- Polanyi model were used to estimate the mean free energy of the adsorption process. This value was

calculated to be 0.04 kJ/ mole, which showed the physical nature of the adsorption process. The heat of the adsorption process was also estimated to be -35.81 kJ/ mol.

According to the dynamic study, the highest content of ethanol in the effluent and separation factor of water to ethanol were achieved at Temperature of 90°C, ethanol feed concentration of 95 wt% and particle size of 0.43- 1.18 mm.

6.2 Recommendations

1- Canola meal after protein extraction has a low selectivity to adsorb water over ethanol. A combination of this biosorbent with other materials can be used to increase the selectivity.
2- Ethanol is adsorbed significantly along with water. The effect of ethanol adsorption could be considered in the adsorption isotherm model.
3- Mathematical modeling could be evaluated to predict the breakthrough curves.
4- The protein extracted canola meal used in this study has a significant amount of protein left. More protein extraction could be carried out to further decrease the amount of protein in the canola meal.
5- The system needs to be modified to decrease the extent of ethanol loss after exiting the bed in the condenser; the regeneration part of the bed could also be enhanced in order to make it possible to measure the adsorbate.
6- Online measurement of the adsorption product and the desorbate contents would lead to more accurate results.

7 References

Al-Asheh, S., F. Banat and N. Al-Lagtah, "Separation of Ethanol–Water Mixtures Using Molecular Sieves and Biobased Adsorbents," *Chem. Eng. Res. Design*. **82**, 855-864 (2004).

Anozie, A.N., E.E. Okuhon, F.N. Osuolale and J.K. Adewole, "Dehydration of Ethanol-Water Mixture Using Activated Carbons from Sawdust and Palm Kernel Shells," *Separation Science and Technology*. **45**, 1482-1489 (2010).

ASTM D 3173-87. Standard method for determination of moisture content in biomass. Philadelphia, PA: Am. Society for Testing Materials, International; (2003).

ASTM D 3174-04. Standard method for ash in the analysis sample of coal and coke. Philadelphia, PA: Am. Society for Testing Materials, International; (2004).

ASTM D 3175-07. Standard method for volatile matter in the analysis sample of coal and coke. Philadelphia, PA: Am. Society for Testing Materials, International; (2007).

Baylak, T., P. Kumar, C.H. Niu and A. Dalai, "Ethanol Dehydration in a Fixed Bed Using Canola Meal," *Energy & Fuels*. **26**, 5226-5231 (2012).

Beery, K.E. and M.R. Ladisch, "Adsorption of Water from Liquid-Phase Ethanol-Water Mixtures at Room Temperature Using Starch-Based Adsorbents," *Ind. Eng. Chem. Res.* **40**, 2112-2115 (2001).

Benson, T.J. and C.E. George, "Cellulose Based Adsorbent Materials for the Dehydration of Ethanol Using Thermal Swing Adsorption," *Adsorption.***11**, 697-701 (2005).

Biagini, E., F. Barontini and L. Tognotti, "Devolatilization of biomass fuels and biomass components studied by TG/FTIR technique," *Ind. Eng. Chem. Res.* **45**, 4486-4493 (2006).

Bienkowski, P.R., A. Barthé, M. Voloch , R.N. Neuman and M.R. Ladisch, "Breakthrough behavior of 17.5 mol% water in methanol, ethanol, isopropanol, and t-butanol vapors passed over corn grits," *Biotechnology and Bioengineering*. **28**, 960-964 (1986).

Canola Council of Canola, Canola Meal Feed Industry Guide.

http://www.canolacouncil.org/uploads/feedguide/Canola_Guide_ENGLISH_2009_small.Pdf, **2012** (2011).

Chang, H., X. Yuan, H. Tian and A. Zeng, "Experiment and prediction of breakthrough curves for packed bed adsorption of water vapor on cornmeal," *Chemical Engineering and Processing: Process Intensification*. **45**, 747-754 (2006).

Chang, H., X. Yuan, H. Tian and A. Zeng, "Experimental Study on the Adsorption of Water and Ethanol by Cornmeal for Ethanol Dehydration," *Ind. Eng. Chem. Res* **45**, 3916-3921 (2006).

Chang, H., X. Yuan, H. Tian and A. Zeng, "Experimental Investigation and Modeling of Adsorption of Water and Ethanol on Cornmeal in an Ethanol-Water Binary Vapor System," *Chem. Eng. Technol.* **29** (2006).

Chowdhury, S., R. Mishra, P. Saha and P. Kushwaha, "Adsorption Thermodynamics, Kinetics and isosteric heat of adsorption of malachite green onto chemically modified rice husk, " *Desalination*. **265**, 159-168 (2011).

Colella, C., M. Pansini, F. Alfani, M. Cantarella and A. Gallifuoco, "Selective water adsorption from aqueous ethanol-containing vapors by phillipsite-rich volcanic tuffs," *Microporous Materials*. **3**, 219-226 (1994).

Cooper, D.C. and F.C. Alley, Eds., "Air Pollution Control," Waveland Press, Inc, The United States of America (2002).

Crawshaw, J.P. and J.H. Hills, "Sorption of Ethanol and Water by Starchy Materials," *Ind. Eng. Chem. Res.* **29**, 307-309 (1990).

Dang, V.B.H., H.D. Doan, T. Dang-Vu and A. Lohi, "Equilibrium and kinetics of biosorption of cadmium (II) and copper (II) ions by wheat straw," *Bioresour. Technol.* **100**, 211-219 (2009).

Diosady, L.L., L.J. Rubin and Y.M. Tzeng, "Production of Rapeseed Protein Materials," *United States Patent*. **43880** (1989).

Fahmi, A., F.A. Banat and R. Jumah, "Vapor-Liquid Equilibrium of Ethanol-Water System in the Presence of Molecular Sieves," *Separation Science and Technology*. **34**, 2355-2368 (1999).

Farooq, U., J.A. Kozinski, M.A. Khan and M. Athar, "Biosorption of heavy metal ions using wheat based biosorbents – A review of the recent literature," *Bioresour. Technol*. **101**, 5043–5053 (2010).

Fogler, H.S., Ed., "Elements of Chemical Reaction Engineering," Prentice- Hall Inc, New Jersey (2006).

Frolkova, A.K. and V.M. Raeva, "Bioethanol Dehydration: State of the Art," *Theoretical Foundations of Chemical Engineering*.**44**, 545-556 (2010).

Ghodsvali, A., M.H.H. Khodaparast, M. Vosoughi and L.L. Diosady, "Preparation of canola protein materials using membrane technology and evaluation of meals functional properties," *Food Res. Int*. **38**, 223-231 (2005).

Gorbach, A., M. Stegmaier and G. Eigenberger, "Measurement and Modeling of Water Vapor Adsorption on Zeolite 4A—Equilibria and Kinetics," *Adsorption.* **10**, 29-46 (2004).

Gulati, M., P.J. Westgate, M. Brewer, R. Hendrickson and M.R. Ladisch, "Sorptive recovery of dilute ethanol from distillation column bottoms stream," *Applied Biochemistry and Biotechnology*.**57/58**, 103-119 (1996).

Hassaballah, A.A. and J.H. Hills, "Drying of ethanol vapors by adsorption on corn meal," *Biotechnology and Bioengineering*. **35**, 598-608 (1990).

Hill, J., E. Nelson, D. Tilman, S. Polasky and D. Tiffany, "Environmental, economic, and energetic costs and benefits of biodiesel and ethanol biofuels," *PNAS***.103**, 11206-11210 (2006).

Hills, J.H. and I.M. Pirzada, "Analysis and prediction of breakthrough curves for packed bed adsorption of water vapor on corn-meal," *Chemical engineering research & design.* **67**, 442-450 (1989).

Himmelsbach, D.S., S. Khalili and D.E. Akin, "The use of FT-IR microspectroscopic mapping to study the effects of enzymatic retting of flax (Linum usitatissimum L) stems," *Science of Food and Agriculture*. **82**, 685-696 (2002).

Hu, X. and W. Xie, "Fixed-Bed Adsorption and Fluidized-Bed Regeneration for Breaking the Azeotrope of Ethanol and Water," *Separation Science and Technology*. **36**, 125-136 (2001).

Jeong, J., B. Jang, Y. Kim, B. Chung and G. Choi, "Production of dehydrated fuel ethanol by pressure swing adsorption process in the pilot plant," *Chemistry and Materials Science*.**26** (2009).

Kaur, R., "Characterization of canola meal for ethanol dehydration," *Internal Report, University of Saskatchewan (*2010).

Khan, A.A. and R.P. Singh, "Adsorption thermodynamics of carbofuran on Sn(IV) arsenosilicate in H^+, Na^+ and Ca^{2+} forms, " *Journal of Colloid science*. **24**, 33- 42 (1987).

Kim, Y., R. Hendrickson, N. Mosier, A. Hilaly and M.R. Ladisch, "Cassava Starch Pearls as a Desiccant for Drying Ethanol," *Ind. Eng. Chem. Res* .**50**, 8678-8685 (2011).

Kumar, S., N. Singh and R. Prasad, "Anhydrous ethanol: A renewable source of energy," *Renewable and Sustainable Energy Reviews*. **14**, 1830-1844 (2010).

Kupiec, K., J. Rakoczy, R. Mirek, A. Georgiou and L. Zielinski, "Adsorption-Desorption Cycles for the Separation of Vapor-phase Ethanol/Water Mixtures," *Adsorption Science & Technology*.**26**, 209-224 (2008).

Kupiec, K., J. Rakoczy and E. Lalik, "Modeling of PSA separation process including friction pressure drop in adsorbent bed," *Chemical Engineering and Processing: Process Intensification*. **48**, 1199-1211 (2009).

Ladisch, M.R. and K. Dyck, "Dehydration of Ethanol: New Approach Gives Positive Energy Balance," *Science.***205**, 898 (1979).

Ladisch, M.R., M. Voloch, J. Hong, P. Blenkowski and G.T. Tsao, "Cornmeal Adsorber for Dehydrating Ethanol Vapors," *Ind. Eng. Chem. Process Des. Dev.* **23**, 437-443 (1984).

Manamperi, W.A., S.W. Pryor and S.K.C. Chang, "Separation and Evaluation of Canola Meal and Protein for Industrial Bioproducts," ASABE Section Meeting Paper No. RRV-07116. St. Joseph, Mich.: ASABE, Fargo, North Dakota, USA, October 12-13, (2007).

Milton Bell, J. and M.O. Keith, "Effect of pig weight and barley hulls on the digestibility of energy, protein and fiber in wheat, corn and hulless barley diets," *Nutr. Res*. **11**, 1307-1316 (1991).

Pitt, J.W.W., G.L. Haag and D.D. Lee, "Recovery of ethanol from fermentation broths using selective sorption–desorption," *Biotechnology and Bioengineering*. **25**, 123-131 (1983).

Poling, B.E., J.M. Prausnitz and J.P. O'Connell, Eds., "The Properties of Gases and Liquids," McGraw-HILL (2001).

Ragauskas, A.J., C.K. Williams, B.H. Davison, G. Britovsek, J. Cairney, C.A. Eckert, W.J. Frederick Jr., J.P. Hallett, D.J. Leak, C.L. Liotta, J.R. Mielenz, R. Murphy, R. Templer and T. Tschaplinski, "The Path Forward for Biofuels and Biomaterials," *Science.***311**, 484-489 (2006).

Raveendran, K., A. Ganesh and K.C. Khilar, "Pyrolysis characteristics of biomass and biomass components," *Fuel.* **75**, 987-998 (1996).

Simo, M., S. Sivashanmugam, C.J. Brown and V. Hlavacek, "Adsorption/Desorption of Water and Ethanol on 3A Zeolite in Near-Adiabatic Fixed Bed," *Ind. Eng. Chem. Res.* **48**, 9247-9260 (2009).

Slejko, F.L., Ed., "Adsorption technology: A step-by-step Approach to Process Evaluation and Application," *Tall Oaks Publishing, Inc*, United States of America (1985).

Sowerby, B. and B.D. Crittenden, "A vapor phase adsorption and desorption model for drying the ethanol-water azeotrope in small columns," *Chemical engineering research & design.***69**, 3-13 (1991).

Sowerby, B. and B.D. Crittenden, "An experimental comparison of type A molecular sieves for drying the ethanol–water azeotrope," *Gas Separation& Purification.* **2**, 77-83 (1988).

Sun, N., C. okoye, C.H. Niu and H. Wang, "Adsorption of Water and Ethanol by Biomaterials," *International Journal of Green energy*.**4**, 623-634 (2007).

Tan, S.H., R.J. Mailer, C.L. Blanchard and S.O. Agboola, "Extraction and characterization of protein fractions from Australian canola meals," *Food Res. Int.* **44**, 1075-1082 (2011).

Thomas, W.J. and B.D. Crittenden, Eds., "Adsorption technology and Design," *Elsevier Science & Technology Books* (1998).

Wang, Y., C. Gong, J. Sun, H. Gao, S. Zheng and S. Xu, "Separation of ethanol/water azeotrope using compound starch-based adsorbents," *Bioresour. Technol*. **101**, 6170-6176 (2010).

Westgate, P.J. and M.R. Ladisch, "Air Drying Using Corn Grits as the Sorbent in a Pressure Swing Adsorber," *Ind. Eng. Chem. Res.* **39**, 720-723 (1993).

Westgate, P.J., J.Y. Lee and M.R. Ladisch, "Modeling of Equilibrium Sorption of Water Vapor on Starch Materials," *Transactions of the ASAE* **.35**, 213-219 (1992).

Wickens, C., "Ethanol dehydration using biosorbents in a pressure swing adsorption process," *Internal Report, University of Saskatchewan* (2010).